



HAL
open science

Revisiting the systematics of flat mites in the genus *Brevipalpus* (Tenuipalpidae): phylogenetic relationships, species groups, taxon delimitation, and cryptic diversity

Renata Santos de Mendonça, Francisco Ferragut, Isis Carolina S. de Oliveira, Aline Daniele Tassi, Felipe Fileni, Ronald Ochoa, Denise Navia

► To cite this version:

Renata Santos de Mendonça, Francisco Ferragut, Isis Carolina S. de Oliveira, Aline Daniele Tassi, Felipe Fileni, et al.. Revisiting the systematics of flat mites in the genus *Brevipalpus* (Tenuipalpidae): phylogenetic relationships, species groups, taxon delimitation, and cryptic diversity. 2025. hal-04907421

HAL Id: hal-04907421

<https://hal.science/hal-04907421v1>

Preprint submitted on 23 Jan 2025

HAL is a multi-disciplinary open access archive for the deposit and dissemination of scientific research documents, whether they are published or not. The documents may come from teaching and research institutions in France or abroad, or from public or private research centers.

L'archive ouverte pluridisciplinaire **HAL**, est destinée au dépôt et à la diffusion de documents scientifiques de niveau recherche, publiés ou non, émanant des établissements d'enseignement et de recherche français ou étrangers, des laboratoires publics ou privés.



Distributed under a Creative Commons Attribution - NonCommercial - NoDerivatives 4.0 International License

1 **Revisiting the systematics of flat mites**
2 **in the genus *Brevipalpus***
3 **(*Tenuipalpidae*): phylogenetic**
4 **relationships, species groups, taxon**
5 **delimitation, and cryptic diversity**

6
7 MENDONÇA RENATA SANTOS¹, FERRAGUT FRANCISCO²,
8 OLIVEIRA ISIS CAROLINA SOUTO DE^{3**}, TASSI ALINE
9 DANIELE⁴, FELIPE FILENI⁵, RONALD OCHOA⁶, NAVIA
10 DENISE ^{7*}

11
12 ¹CAPES/PNPD - Faculdade de Agronomia e Medicina Veterinária, Universidade de Brasília, Campus
13 Universitário Darcy Ribeiro, CEP 70.297-400; Embrapa Genetic Resources and Biotechnology CEP
14 70.770-900, DF, Brasília, Brazil. E-mail mendonca.rsm@gmail.com <https://orcid.org/0000-0002-0514-6442>

15
16
17 ²Instituto Agroforestal Mediterráneo, Universitat Politècnica de València, Camino de Vera, s/n, 46022
18 Valencia, Spain. E-mail fj ferrag@eaf.upv.es <https://orcid.org/0000-0003-1545-6011>

19
20 ³Postgraduate Program in Zoology, Institute of Biological Sciences Universidade de Brasília; Embrapa
21 Genetic Resources and Biotechnology, Cx. Postal 02372, CEP 70.770-900, Brasília, Brazil. E-mail
22 isis.csoliveira@gmail.com <https://orcid.org/0000-0001-7690-5269>

23
24 ⁴Escola Superior de Agricultura "Luiz de Queiroz", Universidade de São Paulo, Cx. Postal 9, CEP
25 13.418-900, Piracicaba, Brazil; University of Florida, Tropical Research and Education Center,
26 Homestead, FL, USA. E-mail alinetassi@gmail.com <https://orcid.org/0000-0002-8622-5977>

27
28 ⁵Newcastle University, School of Engineering, Cassie Building, NE1 7RU, Newcastle Upon Tyne,
29 United Kingdom. E-mail felipef93@gmail.com <https://orcid.org/0000-0001-7260-1946>

30
31 ⁶Systematic Entomology Laboratory, United States Department of Agriculture, Agricultural Research
32 Service, 20705, Beltsville, Maryland, USA. E-mail ron.ochoa@usda.gov <https://orcid.org/0000-0003-1680-3601>

33
34
35 ⁷UMR CBGP, INRAE, CIRAD, Institut Agro, IRD, Univ Montpellier, Institut National de Recherche pour
36 l'Agriculture, l'Alimentation et l'Environnement (INRAE), 755 avenue du Campus Agropolis, CS 30016,
37 34988 Montpellier sur Lez cedex, France. E-mail denise.navia@inrae.fr <https://orcid.org/0000-0003-3716-4984>

38
39
40
41
42
43 **Corresponding author*

44 *Correspondence: E-mail: denise.navia@inrae.fr*

45
46 ***This paper corresponds to part of the Master's research carried out by Isis Carolina Souto de Oliveira*
47 *and presented to the Postgraduate Program in Zoology at the Institute of Biological Sciences,*
48 *Department of Zoology, University of Brasília.*

49

ABSTRACT

Phytophagous mites in the genus *Brevipalpus* (Tenuipalpidae) are important because of their role as vectors of viruses of agricultural importance. However, a phylogeny-based classification to understand their evolution and predict their bioecological aspects is lacking. Accurate species identification is crucial for studying pathosystem interactions, implementing quarantine measures, and developing control strategies. This study aimed to explore the systematics and phylogenetic relationships within the genus *Brevipalpus* by revisiting the species-group classification based on phylogenetic relationships, identifying cryptic species, and determining genetic distance boundaries. A multi-tool exploration of DNA datasets, including mitochondrial (two COI regions) and nuclear (ITS2 and D1-D3), and a detailed morphological study using light and scanning microscopy, was used. Specimens were collected from 20 host plant families from South America, Europe, and the Middle East. Three species-delimitation approaches were applied, namely, Automatic Barcode Gap Discovery (ABGD), Assemble Species by Automatic Partition (ASAP), and a local regression to establish reliable genetic distance thresholds to discriminate different species. Results indicate that the current species-group classification only partially matches that based on genetic lineages. Species currently classified as belonging to the *phoenicis* and *cuneatus* species groups were found to be polyphyletic and related to species currently placed in other species groups. A rearrangement of the species groups to align with the observed genetic lineages is proposed, and morphological traits that are phylogenetically informative are defined. Cryptic diversity in certain taxa was consistently confirmed by various methods. Nuclear and mitochondrial markers were essential for identifying candidate lineages when morphology alone was insufficient. Nuclear markers detected host-associated lineages within certain species. Inconsistencies between markers and methods suggest ongoing speciation processes, and hypotheses about speciation events were explored. Intra- and interspecific genetic distances and threshold values were determined for the four studied genomic fragments and can be used for routine taxonomic identification and uncovering cryptic lineages. Further research should combine genetic data, carefully selected markers, and thorough morphological analysis before proposing new species.

Keywords: False spider mites, phytophagous mites, plant virus vectors, species-delimitation methods, integrative systematics, molecular taxonomy

Introduction

88 Taxonomic classifications based on kinship relationships contribute to the understanding of the
89 evolutionary aspects of organisms, and allow predictions of the biological aspects of a particular
90 taxon based on its shared traits with closely related taxa (Gilbert & Webb, 2007; Kellermann et al.,
91 2012). This phylogenetic background is particularly important for agricultural pests, and is useful
92 for predicting their potential economic impact, their relationship with the phytopathogens they
93 transmit, and for developing control strategies (Kellermann et al., 2012; Godefroid et al., 2016; Jin
94 et al., 2019). However, such background data are still lacking for many important groups of pests,
95 including the phytophagous mites in the genus *Brevipalpus* Donnadieu (Tenuipalpidae).

96 *Brevipalpus* is one of the most diverse genera in the family Tenuipalpidae and currently
97 includes 292 valid taxa (Castro et al., 2024). Species in this genus mainly occur in tropical and
98 subtropical areas, although numerous taxa have also been recorded in the Nearctic, Oriental and
99 Western Palearctic regions (Mesa et al., 2009; Castro et al., 2024). *Brevipalpus* mites cause
100 damage to food crops and ornamental plants because they directly feed in large populations on
101 plant tissues and, to a greater extent, they vectors of plant viruses commonly known as *Brevipalpus*
102 transmitted virus, the citrus leprosis virus (CiLV-C, *Cilevirus leprosis*), and the coffee ring, which
103 are of economic importance (Kitajima et al., 2010; Childers & Rodrigues, 2011). Many new viruses
104 and *Brevipalpus* species acting as vectors are being discovered (de Lillo et al., 2021), and some
105 of these species are officially regulated as quarantine pests in the international exchange or trade
106 of fresh fruit and propagation material of their host plants (Peña et al., 2015).

107 The taxonomy of *Brevipalpus* mites has been a challenge for acarologists for decades. Poor
108 descriptions and illustrations as well as lack of a critical study of their morphology have rendered
109 the taxonomy of the genus difficult (Welbourn et al., 2003; Beard et al., 2015). To put this in context,
110 the species previously considered cosmopolitan in distribution and most reported for virus
111 transmission, *Brevipalpus phoenicis* (Geijskes), has been reclassified as *B. yothersi*, and a species
112 complex has been proposed (Beard et al., 2015) to accommodate the multiple species under the
113 name *B. phoenicis*. Additionally, an integrative approach based on DNA sequences of the
114 mitochondrial *cytochrome c oxidase subunit I (COI)* and a detailed morphological study has been
115 previously used to describe and uncover cryptic species in the genus (Navia et al., 2013; Alves et
116 al., 2019).

117 The genus *Brevipalpus* was divided into species groups by different authors based on a few
118 morphological traits. Baker et al. (1975) and, later, Baker & Tuttle (1987) proposed six species
119 groups -*cuneatus*, *frankeniae*, *californicus*, *obovatus*, *phoenicis*, and *portals*- based on the number
120 of lateral setae on the opisthosoma, the number of solenidia (specialized chemosensory setae) on
121 the female tarsus II, and the number of setae on the distal segment of the palps. These diagnostic
122 criteria have been universally accepted and applied in the taxonomy of the genus for decades;
123 however, the number of solenidia may vary among individuals of the same population and even in
124 the same specimen with the leg of one side bearing one and the opposite side bearing two of these
125 structures (Lindquist, 1985). This supposedly consistent variability in characters has fueled the
126 suspicion that this morphology-based species group is artificial and, therefore, uninformative.
127 Morphological studies examining the characters used to distinguish the species groups, novel
128 taxonomic characters, and DNA analyses, may elucidate these relationships and allow for a
129 redefinition of the species groups based on their phylogenetic relationship.

130 Until now, the mitochondrial gene *COI* has been the only molecular marker used in *Brevipalpus*
131 systematic studies (Groot & Breeuwer 2006; Navia et al. 2013a; Rodrigues et al. 2004; Salinas-
132 Vargas et al. 2016; Sánchez-Velázquez et al. 2015). It has been a valuable tool for studying
133 phylogenetic relationships at lower taxonomic levels (see Navia et al. 2013). However, consistent
134 phylogenies should be based on multiple genes because the use of a single marker only reflects
135 the evolution of that gene and can lead to misinterpretations of the phylogeny. Therefore, use a
136 broader range of molecular markers, including nuclear fragments, may help elucidate the
137 phylogenetic relationships among *Brevipalpus* mites.

138 As in other groups of organisms, delimiting *Brevipalpus* species can be challenging due to the

139 significant intraspecific variability in both morphology (Welbourn et al., 2003) and molecular traits
140 (e.g., Navia et al. 2013a). Integrating DNA-based species-delimitation methods with morphological
141 methods can be useful in clarifying taxonomic uncertainties, especially for closely related or
142 recently diverged species (Jorna et al., 2021) or hyper-diverse groups/taxa (Puillandre, Modica, et
143 al., 2012) undergoing pressures of speciation events (Losos & Mahler, 2010; Czekanski-Moir &
144 Rundell, 2019; Shropshire et al., 2020). Furthermore, establishing intra- and interspecific threshold
145 values could aid in the identification of known species, solve taxonomic issues, and play a crucial
146 role in taxonomic initiatives by highlighting potential new species or cases of cryptic species
147 (Hebert et al., 2004).

148 The main goal of this work was to enhance previous knowledge on the systematics and
149 phylogenetic relationships of the genus *Brevipalpus* by addressing the following objectives: (i) to
150 revisit species-group classification through phylogenetic relationships and evaluating the reliability
151 of the species-group diagnostic characters used in morphological taxonomy; (ii) to check for the
152 occurrence of cryptic species within morphologically recognized species by applying multiple
153 species-delimitation approaches and exploring hypotheses regarding speciation mechanisms and;
154 iii) to establish species genetic distance boundaries based on polynomial regression analysis.

155 **Material and methods**

156 **Specimen collection**

157 Specimens of *Brevipalpus* mites were collected from July 2009 to November 2017 from five
158 countries: Argentina, Brazil, Chile, Israel, and Spain. The details of regions of each country from
159 which specimens were collected are presented in Table 1 and Figure SM1-1.

160 Thirty-three *Brevipalpus* populations were randomly collected from host plants, including fruit
161 trees and ornamental plants, using a 10x hand lens. Samples of leaves and stems from 23 host
162 genera across 20 families of monocotyledon and dicotyledon plants were collected from the field.
163 These samples were transported to the laboratory for further examination under a 40x dissecting
164 stereoscope. Mite individuals collected from the same plant and date in a specific location were
165 considered to be part of the same sample.

166 Specimens of *Brevipalpus* were collected from each sample for morphological studies using
167 light and scanning electron microscopy. Some of the specimens were used for molecular analyses.
168 The specimens used for morphological and molecular analyses were preserved in 70% and 100%
169 ethanol, respectively.

170 **Morphological identification**

171 For light microscopic observations, specimens preserved in 70% ethanol were directly mounted
172 on microscope slides in Hoyer's medium or in polyvinyl alcohol (PVA) medium, before they were
173 kiln-dried at 56°C for 5–7 days. The slide-mounted specimens were observed under a phase and
174 differential interference contrast microscope (Eclipse 80i Nikon, Tokyo, Japan) at 40x and 100x
175 objectives. Specimens were deposited as vouchers in the plant mite collections at the EMBRAPA
176 Recursos Genéticos e Biotecnologia, Brasília, Brazil and of Instituto Agroforestal Mediterráneo,
177 Universidad Politécnica de Valencia, Valencia, Spain (codes are listed in **Table 1**).

178 For scanning electron microscopy, specimens preserved in 100% ethanol were critical point-
179 dried (Leica EM CPD 300), mounted in double-coated carbon tape on stubs, before they were
180 sputter-coated (Baltec SPD 050–Balzers, Lichtenstein). Observations were conducted under a
181 JEOL JSM-IT300 microscope at the Laboratory of Electron Microscopy, ESALQ-USP, in
182 Piracicaba, São Paulo, Brazil.

183 Morphology-based identification was performed using traditional diagnostic traits, such as the
184 number of solenidia (omega, ω) on tarsus II, the presence of opisthosomal setae pair *f*₂, and
185 general dorsal cuticular patterns (Grandjean, 1939; Lindquist, 1985). Additionally, recently valued
186 traits, such as the shape of the spermatheca, type of palp femorogenu seta, detailed dorsal and
187 ventral cuticular patterns, shape of the propodosomal and opisthosomal setae, and leg chaetotaxy,

188 were used (Castagnoli, 1974; Beard et al., 2015). Identification of certain specimens/populations
189 was confirmed by comparing them with the types of each species deposited in the United States
190 National Museum collection (*B. californicus*, *B. papayensis* Baker, *B. phoenicis* [Geijskes], *B.*
191 *mallorquensis* Pritchard & Baker) and EMBRAPA Recursos Genéticos e Biotecnologia (*B.*
192 *incognitus* Ferragut & Navia).

193 **Molecular study**

194 **Genomic region selection**

195 Four target DNA fragments, comprising two mitochondrial and two nuclear, were sequenced to
196 assess the phylogenetic relationships and the genetic variability (intra- and interspecific distances).

197 The two mitochondrial fragments (**Figure SM1-2**), both inside the cytochrome c oxidase I (*COI*)
198 gene were **i)** the 650 bp *COI* corresponding to the “DNA barcoding region” as chosen by the
199 Consortium for the Barcode of Life (<http://barcoding.si.edu>) (Folmer et al., 1994; Hebert et al.,
200 2003), which is among the most widely used barcoding fragments for arthropod groups (Huemer
201 et al., 2014), including Tenuipalpidae (Dowling et al., 2012). The match positions in the
202 mitochondrial genomes of *Brevipalpus yothersi* (Navia et al., 2019) and that of the two-spotted
203 spider mite *Tetranychus urticae* Koch (Tetranychidae) (Van Leeuwen et al., 2008; Grbić et al.,
204 2011) are shown in **Figure SM1-2; ii)** the 400 bp (*COI*) defined by Navajas *et al.* (1996), henceforth
205 referred to as *COI* DNF-DNR. It has been previously used in studies of *Brevipalpus* mites with over
206 300 sequences available in GenBank (Alves *et al.* 2019; Groot & Breeuwer 2006; Navia *et al.*
207 2013a; Rodrigues *et al.* 2004; Sánchez-Velázquez *et al.* 2015) and has been included to link the
208 results obtained herein with those from previous studies. The two selected nuclear genome
209 fragments were **i)** a 1000-bp portion of the large ribosomal RNA subunit (28S gene) spanning the
210 expansion region D1–D3, henceforth referred to as D1–D3. This region has been used for taxon
211 identification and phylogenetic studies from the species level to higher-level diversification of
212 acariform mites (Dowling et al., 2012; Pepato & Klimov, 2015; Alves et al., 2019), and **ii)** a 480-bp
213 fragment spanning the internal transcribed spacers (ITS), including the partial 5,8S gene and the
214 partial ITS2 region. This region, hereinafter referred to as ITS2, has been used in studies dealing
215 with phylogenies, species diagnostics, and cryptic speciation of Tetranychoida, the superfamily
216 in which the family Tenuipalpidae is included (Navajas et al., 1999; Mendonça et al., 2011).

217 **DNA isolation, PCR amplification, and sequencing**

218 Total genomic DNA was extracted from a single adult female using the DNeasy Tissue kit
219 (Qiagen Germantown, MD, USA) according to the DNA extraction protocol “Purification of Total
220 DNA from Animal Blood or Cells” (SpinColumn Protocol), modified for the extraction of mite DNA
221 (Mendonça et al., 2011; Dowling et al., 2012). For each sample, DNA was extracted from 5 to 20
222 specimens. The carcasses of most of the specimens recovered from the last stage of the DNA
223 extraction procedure were intact and were subsequently mounted on slides in Hoyer medium,
224 except for samples from Chile (*Ligustrum* sp. - CH Lisi) and Israel (IS Paed), which contained only
225 a few specimens that could not be retrieved. Recovered specimens were deposited as vouchers
226 in the mite collection of EMBRAPA Genetic Resources and Biotechnology, Brasilia, DF, Brazil.

227 DNA fragments were PCR-amplified in 25 µL reaction volumes containing *Taq* DNA
228 Polymerase, 2.5 µL of 10× PCR buffer, Standard *Taq* buffer (Qiagen, Brazil), and 2 µL of DNA
229 template. All thermocycling profiles included a final elongation step of 10 min at 72°C. PCR primers
230 and reaction conditions are described in **Tables SM2-1** and **SM2-2**. The primer ITS-F was
231 designed in this study.

232 PCR products were resolved by electrophoresis on a 1% agarose gel in 0.5X TBE buffer and
233 visualized on Gel Red staining (Biotium, Inc, Hayward, Canada). The amplified fragments
234 containing visible and single bands were directly sequenced on both strands using an ABI 3730XL
235 (Macrogen, Seoul, Korea). No additional primers were used for the sequencing.

236

Table 1. Collection details of the specimens of *Brevipalpus* mites used in the study.

Morphological identification	Host plant		Locality	Latitude, Longitude	Collector	Date	Slides (NSPS)*	Voucher code
	Scientific and common name	Family						
<i>B. yothersi</i>	<i>Citrus sinensis</i> (sweet orange)	Rutaceae	Rearing population genome sequence***	15° 43' 52", 47° 54' 08"	Navia D., Novelli V.M.	05.ix.2015	5 (5)	BRDF Cisi
<i>B. yothersi</i>	<i>Ipomoea batatas</i> (sweet potato)	Convolvulaceae	Arapiraca, AL, Brazil	09° 45' 09", 36° 39' 40"	Navia D., Silva E.S.	v. 2013	10 (50)	BRAL Ipba
<i>B. yothersi</i> ; <i>B. n. yothersi</i> 1* <i>B. n. californicus</i> 1	<i>Hibiscus rosa-sinensis</i> (hibiscus)	Malvaceae	UFRPE, Recife, PE, Brazil	8° 0' 53.14", 34° 56' 59.16"	Gondim Jr M.G. C., Navia D.	27.vii.2012	8 (40)	BRPE Hiro
<i>B. yothersi</i> <i>B. incognitus</i>	<i>Phoenix</i> sp. (date palm)	Arecaceae	Piracicaba, SP, Brazil	-22° 43' 31", -47° 38' 57"	Kitajima E.W.	31.v.2013	2 (10)	BRSP Phsp
<i>B. yothersi</i> <i>B. n. yothersi</i> 2	<i>Delonix regia</i> (flamboyant)	Fabaceae	Piracicaba, SP, Brazil	-22° 43' 31", -47° 38' 57"	Kitajima E.W.	02.vi.2013	3 (15)	BRSP Dere
<i>B. yothersi</i>	<i>Cecropia pachystachya</i> (ambay)	Cecropiaceae	Guajará Mirim, RO, Brazil	10° 24' 4.96", 65° 24' 51.94"	Navia D., Ferragut F.	ix. 2012	1 (5)	BRRO Cepa
<i>B. yothersi</i>	<i>Citrus clementine</i> (common clementine)	Rutaceae	Bella Vista, Corrientes, Argentina	34° 33' 49.34", 58° 41' 25.43"	Kitajima E.W.	26.xi.2013	2 (10)	AR Cidl
<i>B. yothersi</i> <i>B. new sp.</i>	<i>Citrus sinensis</i> (sweet orange)	Rutaceae	Bella Vista, Corrientes, Argentina	34° 33' 49.34", 58° 41' 25.43"	Kitajima E.W.	26.xi.2013	3 (15)	AR Cisi
<i>B. yothersi</i>	<i>Passiflora edulis</i> (passion fruit)	Passifloraceae	Israel	unknown	Ben David T.	26.xi.2013	1 (5)	IS Paed
<i>B. n. yothersi</i> 2 <i>B. lewisi</i>	<i>Citrus sinensis</i> (sweet orange)	Rutaceae	Palma del Rio, Cordoba, Spain	+37° 41' 58.72", 5° 16' 51.00"	Ferragut F.	x. 2011	1 (5)	ES Cisi
<i>B. incognitus</i>	<i>Annona muricata</i> (soursop)	Annonaceae	Bonfim, RR, Brazil	+03° 21' 36", 59° 49' 59"	Navia D.	15.vii.2009	8 (40)	BRRR Anmu
<i>B. incognitus</i>	<i>Cocos nucifera</i> (coconut)	Arecaceae	Pacaraima, RR, Brazil	+04° 25' 52", 61° 08' 46"	Navia D.	14.vii.2009	4 (20)	BRRR Conu
<i>B. n. incognitus</i> 1 <i>B. n. incognitus</i> 2	<i>Cocos nucifera</i> (coconut)	Arecaceae	UNIMONTES, Janaúba, MG, Brazil	15° 50' 18.60", 43° 24' 48.11"	Alves R. de B. das N.	ix. 2012	10 (50)	BRMG Conu
<i>B. californicus</i> ss; <i>B. lewisi</i>	<i>Vitis vinifera</i> (grape)	Vitaceae	Ademuz, Valencia, Spain	+40° 03' 45", 1° 17' 04"	Ferragut F., Navia D.	19.x.2014		ESBwA
<i>B. californicus</i> ss; <i>B. lewisi</i>	<i>Citrus lemon</i> (lemon)	Rutaceae	Elche, Alicante, Spain	+38° 17' 28", 0° 36' 20"	Ferragut F., Navia D.	20.x.2014		ESBcE
<i>B. californicus</i> ss <i>B. ferraguti</i>	<i>Pittosporum tobira</i> (japanese cheesewood)	Pittosporaceae	Valencia, Spain	+39° 30' 3.10", 0° 22' 15.66"	Ferragut F., Navia D.	1.x.2011	2 (10)	ES Pito
<i>B. lewisi</i>	<i>Vitis vinifera ssp. sylvestris</i> (grape)	Vitaceae	Ademuz, Valencia, Spain	+40° 03' 51", 1° 16' 49"	Ferragut F., Navia D.	19.x.2014		ESBwC

Table 1. Continued ...

Morphological identification	Host plant		Locality	Latitude, Longitude	Collector	Date	Slides (NSPS)*	Voucher code
	Scientific and common name	Family						
<i>B. phoenicis</i>	<i>Citrus</i> sp. (orange)	Rutaceae	Ibiuna, SP, Brazil	23° 37' 27", 47° 19' 55"	Kitajima E.W.	11.iv.2017	1(4)	109_Cisp_I BI_SP
<i>B. papayensis</i>	<i>Coffea arabica</i> (coffee)	Rubiaceae	Campinas, SP, Brazil	22° 42' 30.3", 47° 37' 53.8"	Tassi A.D.	24.xi.2017	1(1)	123_Coar_ CAM_SP
<i>B. papayensis</i>	<i>Coffea</i> sp. (coffee)	Rubiaceae	Campinas, SP, Brazil	22° 42' 30.3", 47° 37' 53.8"	Tassi A.D.	24.xi.2017	1(4)	124_Cosp_ CAM_SP
<i>B. papayensis</i> <i>B. obovatus</i>	<i>Ligustrum sinense</i> (Chinese privet)	Oleaceae	Brazil, DF, Brasilia	47° 87' 00", 15° 77' 00"	Mendonça, R.S.	12.i.2006		BRDF Lisp
<i>B. ferraguti</i>	<i>Tecomaria capensis</i> (Cape-honeysuckle)	Bignoniaceae	Valencia, Spain	+39° 30' 3.10", 0° 22' 15.66"	Ferragut F., Navia D.	1.x.2011	2 (10)	ES Teca
<i>B. ferraguti</i>	<i>Myoporum laetum</i> (ngaio tree)	Scrophulariaceae	Valencia, Spain	+39° 30' 3.10", 0° 22' 15.66"	Ferragut F., Navia D.	1.x.2011	2 (10)	ES Myla
<i>B. obovatus</i>	<i>Solanum violifolium</i> ** (creeping violet)	** Solanaceae	rearing population ESALQ, Piracicaba, SP, Brazil	-22° 43' 31", -47° 38' 57"	Kitajima E.W.	28.v.2013	2 (10)	BRSP Sovi
<i>B. obovatus</i>	<i>Helichrysum stoechas</i> (everlasting flower)	Asteraceae	El Saler, Valencia, Spain	+39° 22' 57.00", 0° 19' 57.00"	Navia D., Ferragut F.	13.x.2013	5 (25)	ES Hest
<i>B. obovatus</i>	<i>Coniza bonariensis</i> (flaxleaf fleabane)	Asteraceae	El Saler, Valencia, Spain	+39° 22' 57.00", 0° 19' 57.00"	Navia D., Ferragut F.	13.x.2013	6 (30)	ES Cobo
<i>B. chilensis</i>	<i>Magnolia grandiflora</i> (majestic beauty)	Magnoliaceae	San Francisco de Mostazal, Cachapoal, Chile	33° 54' 58.38", 70° 40' 31.22"	Trincado R.	18.ii.2013	1 (5)	CHT Mggr
<i>B. chilensis</i>	<i>Ligustrum sinense</i> (Chinese privet)	Oleaceae	Curacavi, Santiago, Chile	33° 28'9.80", 70° 43' 26.14"	Trincado R.	28.ii.2013	1 (5)	CH Lisi
<i>B. chilensis</i>	<i>Magnolia grandiflora</i> (majestic beauty)	Magnoliaceae	San Francisco de Mostazal, Cachapoal, Chile	33° 54' 58.38", 70° 40' 31.22"	Kitajima E.W.	08.v.2014	1 (5)	CH Mggr
<i>B. chilensis</i>	<i>Ribes punctatum</i> (Chilean currants)	Grossulariaceae	Parque Fray Jorge, Limarí, Chile	33° 37'6.21", 70° 42' 25.40"	Kitajima E.W.	08.v.2014	1 (5)	CH Ripu
<i>B. mallorquensis</i>	<i>Rosmarinus officinalis</i> (rosemary)	Lamiaceae	Úmbria de los Fresnos (Mijares), Valencia, Spain	+39° 28' 11.67", 0° 22' 34.64"	Navia D., Ferragut F.	12.x.2013	2 (10)	ES Roof
<i>B. n. mallorquensis</i>	<i>Erica</i> sp. (heather honey)	Ericaceae	Almedijar, Sierra de Espadan, Castellon, Spain	+39° 55' 8.18", 0°23' 37.22"	Navia D., Ferragut F.	09.vii.2013	6 (30)	ES Ersp
<i>B. oleae</i>	<i>Olea europea</i> (olive tree)	Oleaceae	Jardin del Real, Valencia, Spain	+39° 28' 50.74", 0° 22' 3.78"	Navia D., Ferragut F.	16.x.2013	1 (5)	ES Oleu

238 * NSPS = Number of slides and specimens (in parenthesis) per population/sample; * n. = near, putative species disclosed by the diagnostic information

239 ** *Solanum violifolium* [= *Lycianthus asarifolia*]

240 *** Population from the rearing used to sequencing and assembly the whole-genome of *Brevipalpus yothersi* (Navia *et al.* 2019)

241 **Dataset and sequence retrieval**

242 The dataset comprised 399 *Brevipalpus* sequences of the four selected DNA fragments used
243 in this study. The distribution of the sequences per fragment is shown in **Table SM2-3**. Sequences
244 were also retrieved from GenBank, and their accession numbers and respective authors are shown
245 in **Table SM2-4**. Basically only *COI* (DNF-DNR) sequences of *Brevipalpus* (328) were available in
246 GenBank, except for one sequence for the subunit D1-D3 (Accession number KP276421) (Pepato
247 & Klimov, 2015) and one from ITS2 (HE984346) (unpublished data). To ensure the accuracy of
248 the dataset, as highlighted by Mendonça *et al.* (2011) for Tetranychidae mites, only sequences
249 from peer-reviewed journals with information on the diagnostic identification methods for the
250 specimens were retrieved from GenBank. Two unpublished ITS2 sequences—*Brevipalpus*
251 *phoenicis* HE984346 and *Raoiella macfarlanei* KP318126—were included in the datasets after
252 confirming their correct assignment. The relationship between these query sequences and their
253 neighboring reference sequences was confirmed using a Neighbor-Joining tree and the Kimura 2-
254 parameter (K2P) distance algorithm (Hebert *et al.*, 2003; Austerlitz *et al.*, 2009). Additionally, a
255 BLAST search in GenBank was conducted to check the accuracy of *COI* (DNF-DNR), the subunit
256 D1-D3, and the ITS2 sequences using other sequences of *Brevipalpus* species (Groot & Breuwer,
257 2006; Navia *et al.*, 2013; Sánchez-Velázquez *et al.*, 2015; Pepato & Klimov, 2015; Alves *et al.*,
258 2019). The sequences of the *COI* barcoding were aligned with those of *Raoiella indica* (Dowling *et al.*,
259 2012) because this fragment was herein sequenced for the first time for *Brevipalpus*. The DNA
260 sequences of two other genera of Tenuipalpidae, namely, *Cenopalpus* and *Raoiella*, obtained in
261 this study and retrieved from GenBank, were used in the phylogenetic analysis as sister and out-
262 group, respectively (**Tables SM2-3 and 4**).

263 The putative species identified through diagnostic information (morphological traits,
264 phylogenetic analysis, and delimitation methods) received the interim name of its closest species
265 preceded by the prefix "near" and followed by a sequential number in ascending order, for example,
266 *B. near yothersi* 1 and *B. near yothersi* 2 or simply *B. near mallorquensis*, abbreviated as *B. n.*
267 *yothersi* 1, and so on. The new species in branches without closely related taxa were designated
268 as *Brevipalpus* new sp (*B. new sp.*). Further taxonomic studies presenting complete species
269 descriptions will be conducted to assign scientific names to these putative new taxa.

270 **Sequence edition and alignments**

271 The Staden Package v.1.6.0 (Staden *et al.*, 1998) was used for checking the quality, editing,
272 and assembling the raw data into sequence contig. The DNA sequences were aligned by the
273 ClustalW multiple alignment procedure using BIOEDIT 7.0 (Hall, 1999) and Muscle (Muscle:
274 multiple sequence alignment comparison by log–expectation program) (Edgar, 2004). No manual
275 adjustments of the alignments were made. The alignment of *COI* sequences was confirmed by
276 translating the aligned DNA into amino acids using the Expsy server,
277 <https://web.expasy.org/translate/> (Gasteiger, 2003). To identify candidate protein-coding regions
278 in DNA sequences, an open reading frame was determined using the graphical analysis tool (ORF
279 FINDER) available at <https://www.ncbi.nlm.nih.gov/orffinder/>. The Smart BLAST tool in the
280 National Center for Biotechnology Information
281 (<https://blast.ncbi.nlm.nih.gov/smartblast/smartBlast.cgi>) was used to detect aberrant or unusual
282 sequences.

283 Nucleotide composition (calculated as the base frequencies for each sequence and an overall
284 average), substitution patterns, and rates were estimated using jModeltest version 2.1.10
285 20160303 (Darriba *et al.*, 2012) according to the selected model (**Table SM2-5**). The homogeneity
286 of the substitution patterns between sequences was tested with the Disparity Index (ID).

287 **Phylogenetic analysis**

288 To determine the phylogenetic relationship among taxa, various analytical methods were used
289 including the Maximum Likelihood (ML), Neighbor Joining (NJ), and Bayesian Inference (BI). For

290 ML analyses, the jModeltest was used to estimate the best-fit nucleotide substitution models using
291 the Akaike information criterion corrected (AICc) and the Bayesian information criterion for each
292 dataset. The proportion of invariable sites (I) and gamma-distributed rates (G) defined in the
293 jModeltest were conserved in all models. The best-fit models as well as information on the ML
294 parameters are shown in **Table SM2-5**.

295 The ML analyses were also performed using the online version of PhyML v. 3.0 (Guindon &
296 Gascuel, 2003; Guindon et al., 2010), and NJ analysis was performed using MEGA 7.0 (Kumar et
297 al., 2016). NJ trees were constructed by treating gaps as missing data. The Bayesian Information
298 analysis was performed using MrBayes V.3.2.6 (Ronquist et al., 2012). The topologies of the trees
299 obtained using ML, NJ, and BI were compared. The robustness of the trees was assessed with a
300 bootstrap analysis with 1,000 replicates. Topologies with posterior probabilities of 0.95 were
301 regarded as well supported (Wilcox et al., 2002).

302 The distributions and frequencies of haplotypes (*COI* fragments) and sequence variants
303 (genotypes) (D1–D3 and ITS2) were inferred using DnaSP version 6 (Rozas et al., 2017). When
304 identical sequences were found in the alignment, *i.e.*, sequences sharing a common
305 haplotype/genotype, a single sequence of each group was included in the alignment to produce
306 the ML tree, and the number of times the identical sequences occurred in the dataset was indicated
307 in brackets in the phylogenies.

308 **Bayesian Combined Analysis**

309 To perform the Bayesian Combined Analysis (BCA), unique variants (haplotypes/genotypes)
310 of the nucleotide sequences of each fragment were concatenated according to the *Brevipalpus*
311 clusters observed in the output files of the ML individual gene tree analyses. Any *Brevipalpus*
312 specimen for which fewer than two fragments were sequenced was excluded.

313 The concatenated sequences were achieved for three sets: i) a complete DNA set, including
314 the four fragments (two mitochondrial and two nuclear); ii) the two mitochondrial *COI* fragments,
315 and iii) the two nuclear fragments. The sequence files were individually organized using MEGA
316 v.7. Alignment of the four fragments was performed separately with the software Muscle v3.8.31.
317 The files containing 19 *Brevipalpus* taxa were concatenated in three matrices (complete,
318 mitochondrial, and nuclear) in Mesquite v.3.0.4 (a modular system for evolutionary analysis)
319 (Maddison & Maddison, 2021). The complete set alignment had 74 sequences totaling 2,653 base
320 pairs (bps) (*COI* barcoding = 661 bps; *COI* DNF–DNR = 369 bps; D1–D3 = 1,001 bps; ITS2 = 622
321 bps), and the mitochondrial and nuclear set alignments had 60 sequences/1030 bp and 51
322 sequences/1623bp, respectively.

323 The BCA was performed in MrBayes v.3.2. The number of categories used to approximate the
324 gamma distribution was set at four, and four Markov chains were run for 10,000,000 generations;
325 the final average standard deviation of the split frequencies was less than 0.01, and the
326 stabilization of the model parameters (burn-in = 0.25) occurred at approximately 250 generations.
327 The phylogenetic trees, based on the MrBayes output file (Newick format) created by the PhyML
328 3.0 algorithm and MrBayes program, were edited using FigTree v.1.4.3 ([http://
329 tree.bio.ed.ac.uk/software/figtree/](http://tree.bio.ed.ac.uk/software/figtree/)) (Rambaut, 2009). The alignments can be provided upon
330 request.

331 **Exploring genetic distances to support species identification**

332 Analyses of the overall pairwise genetic distances (distribution and frequencies) and between
333 nucleotide sequences were performed for each DNA fragment using MEGA v. 7 (Kumar et al.,
334 2016). The analyses of intra- and interspecific divergences were explored among the taxa
335 assignments based on multiple methods, including: **i)** the classical distance threshold-based
336 approach used to elaborate distance matrices between intra- and interspecific distances; **ii)** DNA-
337 based species-delimitation performed using Automatic Barcode Gap Discovery (ABGD)
338 (Puillandre, Lambert, et al., 2012); **iii)** Assemble Species by Automatic Partitioning (ASAP)
339 (Puillandre et al., 2021), and **iv)** intra- and interspecific thresholds based on polynomial regression

340 fitting.

341 The genetic distance values were analyzed and compared with the observed morphological
342 divergences between close and putative species, searching for a link for these three approaches
343 (genetic distance, phylogeny, and morphology). The distance matrices were constructed using the
344 Kimura 2-parameter model (K2P) (Kimura, 1980) and uncorrected p -distance, and the standard
345 error estimates were obtained using a bootstrap procedure (1,000 replicates) in MEGA v.7. The
346 K2P model was first used to make these results suitable for comparison with previous studies on
347 Acari, such as Tetranychidae (Mendonça et al., 2011; Sakamoto et al., 2017), Eriophyidae
348 (Skoracka et al., 2012) and Phytoseiidae (Lima et al., 2018). Genetic distances are usually
349 calculated without models selected for specific data (Strimmer *et al.* 2009; and Srivathsan & Meier,
350 2012). A simple distance measure was implemented to improve estimates of intra- and interlineage
351 genetic variation, as in the studies of invertebrate diversity (Collins et al., 2012). Therefore, the
352 uncorrected p -distances with SE estimates (bootstrap procedure 1,000 replicates) were also
353 accessed using MEGA 7.

354 Species hypotheses based on intra- and inter-diversities for closely related taxa

355 The intra- and interspecific genetic distance (K2P and p -distances) values between *Brevipalpus*
356 species, including the putative species, were calculated to explore the values that separate one
357 taxon from another.

358 Scenarios and hypotheses were evaluated to estimate the distance values, *i.e.*, the genetic
359 distances for various taxa combinations, considering: **i)** the morphological similarities and **ii)** the
360 architecture revealed by the phylogenetic tree topologies obtained through the BCA (**Figures 1,**
361 **2A, and 2B**), as well as through the ML phylogenies performed separately for each fragment
362 (**Figures SM1-3–SM1-6**). There was a convergence of the analyzed hypotheses and the clades
363 revealed by phylogeny; therefore, only the results related to the clusters revealed by the
364 concatenated phylogeny will be discussed.

365 The distance matrices within and between *Brevipalpus* species were processed as follows: **i)**
366 mean distance values; **ii)** the maximum and minimum values observed within the same species
367 (intraspecific variation), and **iii)** the maximum and minimum values observed between two species
368 (interspecific variation). Minimal interspecific variation is assumed to be the Nearest Neighbor
369 according to Kekkonen *et al.* (2015). For each fragment, the lowest reliable genetic divergences
370 between taxa with clearly different taxonomic statuses, *e.g.*, *B. chilensis* versus *B. obovatus*, were
371 used to guide assumptions regarding the taxonomic status of the putative species, as indicated by
372 the combined phylogenies and morphological observations (Navia et al., 2013).

373 DNA-sequence-based species-delimitation method

374 The ABGD algorithm was used to determine the occurrence of various species within a dataset
375 based on the gap between clusters of sequence pairs (Puillandre, Lambert, et al., 2012) on the
376 web interface (<https://bioinfo.mnhn.fr/abi/public/abgd/abgdweb.html>). To investigate a range of
377 partitions from conservative to liberal species-delimitation schemes, three values of the relative
378 gap width ($X = 1.0, 1.25, 1.5$) were tested, and two distance metrics were used (K2P and p -
379 distance). For the range of prior intraspecific divergences (P), the sampled values were estimated
380 from $P_{\min} = 0.001$ to $P_{\max} = 0.1$. Defaults were used for all other parameter values. Prior intraspecific
381 divergence (P) ranged from 0.001 to 0.1, with steps set to 10 and Nr bins (for distance distribution)
382 set to 20. Parameters for ABGD were analyzed to select those whose results better matched
383 known species. ABDG analyses were performed per *Brevipalpus* species that were clustered in
384 clades identified by phylogeny.

385 The ASAP (Puillandre et al., 2021) was used to detect the hypothesized partitions of the
386 species and the *Brevipalpus* species boundaries. Multiple sequence alignments were analyzed
387 using ASAP Web Server (<https://bioinfo.mnhn.fr/abi/public/asap/asapweb.html>), with the “ASAP-
388 score” and the probability value considered to select the optimal number of species partitions, as
389 well as the partitions within the range of genetic distances of 0.005 and 0.05, regarding the K2P

390 and simple distance (p -distances). The ASAP analysis was performed using the complete set of
391 sequences per fragment.

392 Intra- and interspecific thresholds based on the polynomial regression fitting

393 Intra- and interspecific genetic divergences for the four DNA fragments were examined for a
394 finer characterization of the levels of divergence among species (Robinson et al., 2009). The
395 analyses were elaborated using both the morphospecies and the putative species (19 taxa) to
396 define reliable threshold values to discriminate the taxa studied here. Two distance types were
397 computed: the maximum intradifference observed within the same species (maximal intraspecific
398 variation) and the minimum interdifference observed between two species of the same genus
399 (minimal interspecific variation), assumed to be the Nearest Neighbor (Kekkonen et al., 2015)
400 using the species selected from the database. Intradifferences were sorted in descending order
401 whereas interdifferences were sorted in ascending order. The position of each point was divided
402 by the sample size, resulting in two curves with values distributed between 0 and 1 for comparison.
403 For instance, the *COI* barcoding region had 136 interdifference values that were ordered in
404 descending order. The minimum difference between *B. oleae* and *B. ferraguti* was 18.2%, and was
405 the thirteenth largest difference among species; therefore, the *B. oleae*-*B. ferraguti* difference was
406 represented by the point: $x = 13/136 = 0.095$ and $y = 0.182$. A margin of error for each point was
407 obtained based on the standard error of the sample and a significant threshold of $\alpha < 0.05$.

408 The focus was on the intersection between the curves of the intra- and interspecific values and
409 the position where the interspecific values were higher than the intraspecific ones. As both curves
410 were modeled with points that presented a margin of error instead of a point of intersection, the
411 curves have an ambiguous zone where the intra- and interspecific values cannot be differentiated
412 at the previously defined significance level (**Figure SM1-7**). The modeling of intra- and interspecific
413 values was performed with a local polynomial regression fitting (Savitzky & Golay, 1964). Use of
414 nonlocal regressions, such as linear, exponential, and logarithmic regression, resulted in a
415 goodness-of-fit that was often less than 0.8. The analysis presents a convergence area, as a
416 polygon, where the closest species are mixed (**Figure SM1-7**). Within this area, it is challenging to
417 delineate species based solely on genetic distance criteria, as some intraspecific values overlap
418 or even match up with interspecific values, violating the gap concept of the barcoding premise
419 (Hebert et al., 2003; Meyer & Paulay, 2005). The overlap of these values could represent
420 incompletely sampled groups, particularly when the coalescent process has not fully sorted
421 between incipient species (ancestral polymorphism), giving rise to genetically polyphyletic or
422 paraphyletic species (Rosenberg, 2003). The intersection point (y) in the convergence area
423 represents the average value where the intraspecific distance meets the interspecific distance.
424 Values that escape the gap (where differences within a species reach high values exceeding the
425 minimum value found between two different species, α) were regarded as *threshold guide values*
426 to drive diagnostic studies. Genetic distance values within the confidence interval suggest possible
427 co-specificity, whereas values above the upper limit indicate different taxa. The threshold-based
428 approach was applied to indicate a reliable distance interval where there was no overlap of
429 *Brevipalpus* intra- and interspecific distance values, especially when dealing with a large set of
430 DNA sequences.

431 **Results**

432 **Datasets, haplotypes, and sequence diversity indexes**

433 The datasets of the four DNA fragments consisted of 2,653 base pairs (bp) of nucleotides, with
434 1,030 bp from the mitochondrial *COI* barcoding region ($\cong 650$ bp), *COI* DNF–DNR ($\cong 364$ bp), and
435 1,623 bp from the nuclear ribosomal regions, including subunit D1–D3 ($\cong 1,000$ bp) and ITS2 ($\cong 480$
436 bp). The number of sequences analyzed varied between fragments, with the most frequent being
437 those of *COI* DNR–DNF (432 sequences), followed by those of ITS2 (118), D1–D3 (97), and *COI*
438 barcoding (84) (**Table SM2–3**).

439 The assigned species names, DNA sequence variation (haplotypes, genotypes), number of
440 times sequences occurred in the dataset (frequency), and respective GenBank accessions are
441 shown for each fragment in **Tables SM2–6 - 9** for *COI*- barcoding, *COI* DNF-DNR, subunit D1–
442 D3, and ITS2, respectively.

443 Intraspecific comparison of genetic diversity indices was estimated for each fragment (**Table**
444 **SM2-10**). The number of variable sites, the average number of differences in nucleotides (K), and
445 the diversity of nucleotides (*Pi*) showed high variability in the mitochondrial and nuclear sequences.
446 Nucleotide diversity (*Pi*) ranged from 5.52% to 9.09% and from 6.24% to 12.58% for the
447 mitochondrial and nuclear fragments, respectively. The average number of differences in
448 nucleotides (K) and nucleotide diversity (*Pi*) showed high variability in the mitochondrial and
449 nuclear sequences of *Brevipalpus* taxa.

450 **Molecular phylogeny of the *Brevipalpus* species**

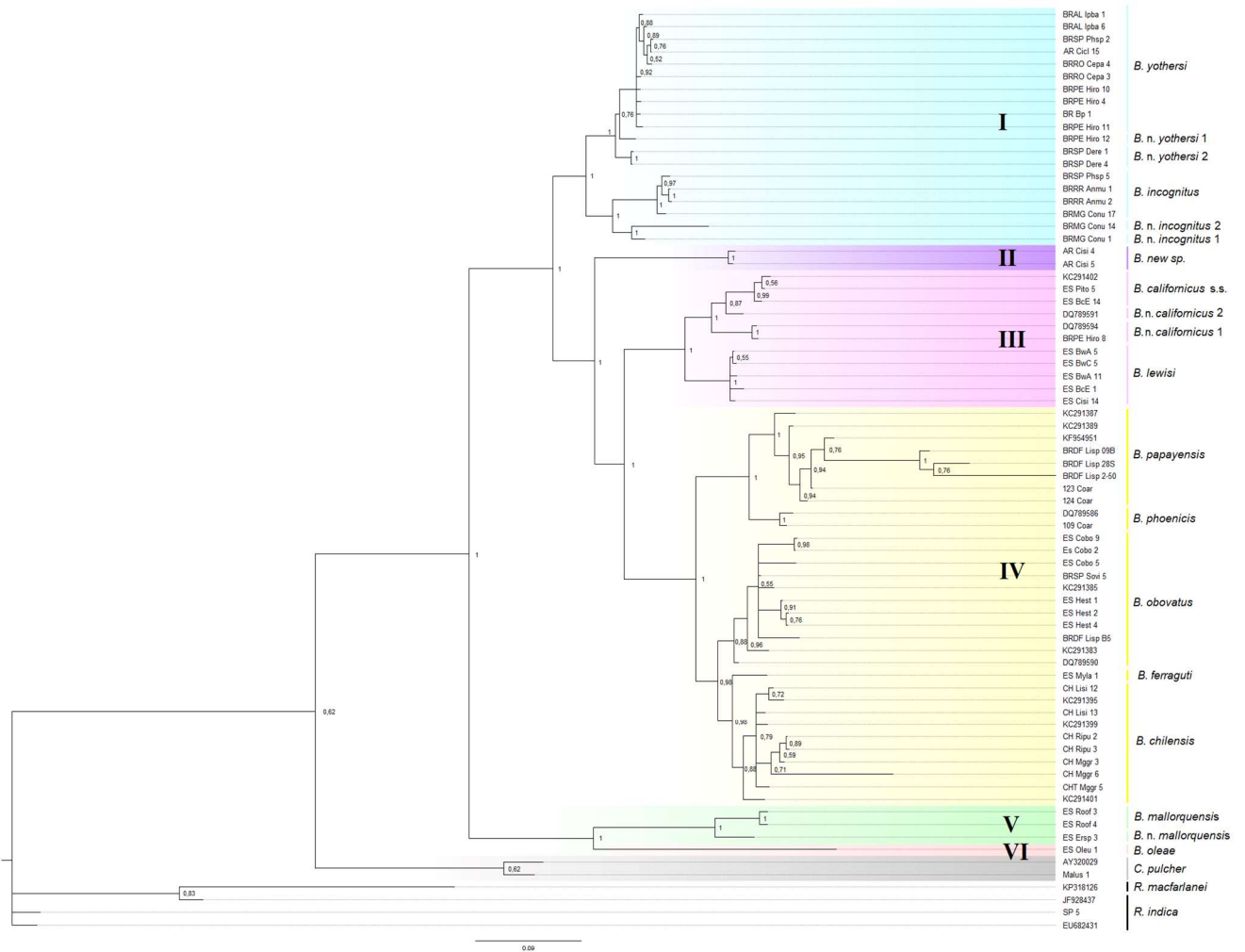
451 The general topologies of the phylogenetic trees inferred by the NJ, ML analyses, and BI were
452 congruent and revealed a similar pattern for all four fragments. Thus, only the ML phylogeny is
453 shown for each fragment. The BCA phylogeny-based on the complete DNA dataset produced a
454 well-supported tree (**Figure 1**). Nodes representing the closest relationships had a Bayesian
455 posterior probability (BPP) of one, and were also consistently recovered by the ML methods for
456 each fragment individually (**Figures SM1-3 - 6**).

457 Phylogenetic analysis grouped the *Brevipalpus* species/putative species into six main clades:
458 **I**-*Brevipalpus yothersi*, *B. near yothersi* 1, *B. near yothersi* 2, *B. incognitus*, *B. near incognitus* 1,
459 and *B. near incognitus* 2; **II**-*Brevipalpus* n. sp., composed of only specimens collected from *Citrus*
460 from Argentina; **III**-*B. californicus* s.s., *B. near californicus* 1, *B. near californicus* 2, and *B. lewisi*;
461 **IV**-*B. phoenicis*, *B. papayensis*, *B. ferraguti*, *B. obovatus*, and *B. chilensis*; **V**-*B. mallorquensis* and
462 *B. near mallorquensis*, and **VI**-consisting of only *B. oleae*. The deepest node clustered clades I, II,
463 III, and IV, whereas another one clustered clades V and VI. The deepest node separated the
464 species in Clade I from the three remaining groups. Clades III and IV grouped as a lineage with a
465 common ancestor.

466 The tree based on the concatenated mitochondrial sequences (**Figure 2A**) generally agrees
467 with the tree based on the complete DNA set. Most nodes were highly supported, except for the
468 clustering of clades III and IV, which had a support value of BPP = 0.81 (compared to BPP = 1 for
469 the complete combined tree). For the tree based on the concatenated nuclear regions (**Figure 2B**),
470 most of the basal nodes were well supported (BPP ≥ 0.99). However, with the tree based on the
471 concatenated nuclear regions was different in structure from the one based on the complete
472 dataset in that Clade II was nested with Clade I making a weakly supported node (BPP = 0.61). In
473 contrast, clades III and IV both showed high support (BPP = 1) in the complete DNA dataset and
474 concatenated *COI*.

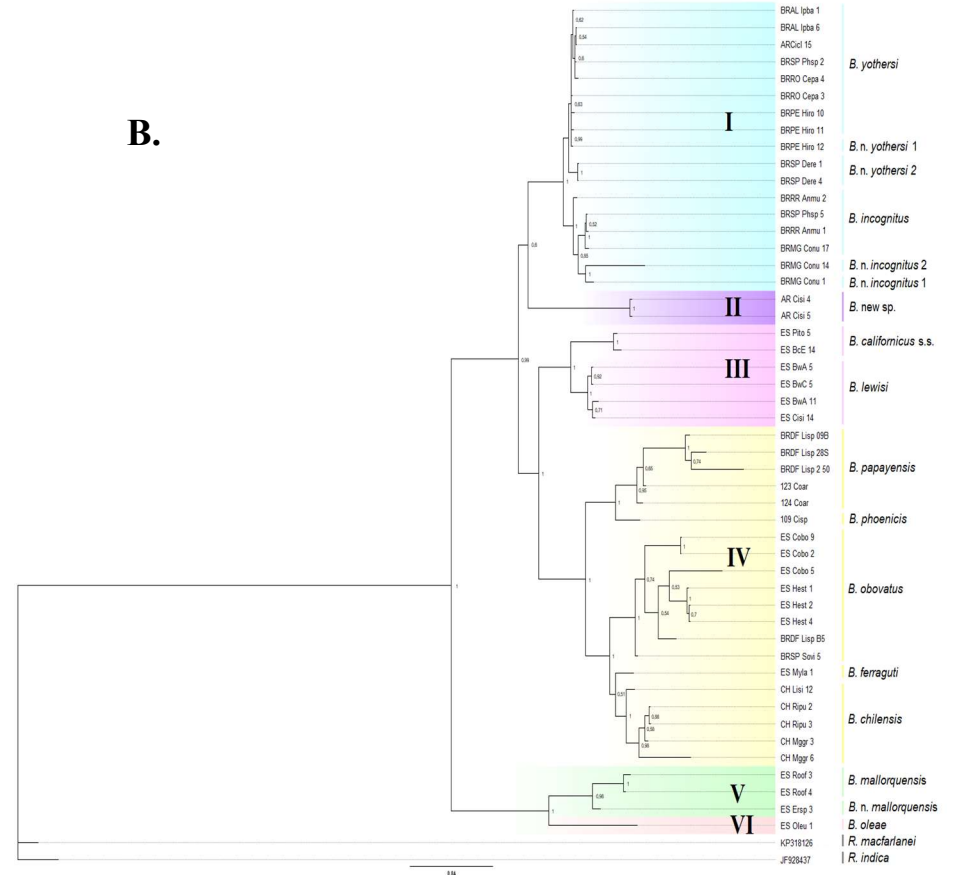
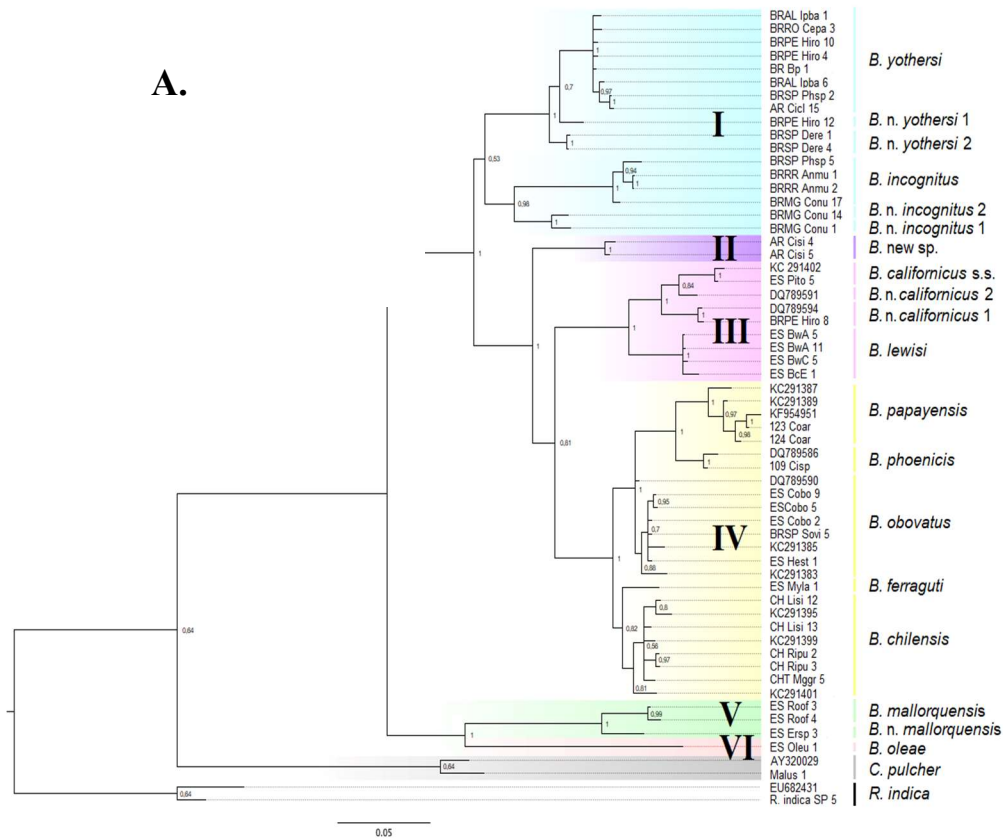
475 The species and putative species and the hypothesized new species shown by the phylogenies
476 (CBA and ML) obtained for each fragment are summarized in **Table 2**. The taxa observed
477 throughout the phylogenies were congruent and converged to a similar number of assigned
478 species, taking into account the missing sequences. Eleven species were recorded for the *COI*
479 fragments and the subunit D1–D3. For the ITS2 region, the dataset included ten species, as no
480 sequences of *B. oleae* were obtained. The number of putative species uncovered by the
481 phylogenies differed among the fragments because for some taxa no sequences were obtained
482 for some fragments (**Table 2**).

483
484
485
486
487
488
489
490



491
492
493
494
495
496
497
498
499
500
501
502
503
504
505
506
507

Figure 1. Combined Bayesian inference (BI) tree analysis for *Brevipalpus* species reconstructed from four genomic fragments: the mitochondrial *cytochrome c oxidase subunit I* (*COI*) (*COI* barcoding region and *COI* DNF–DNR), the ribosomal subunit D1–D3 in the 28S gene (D23F & D6R primers), and the internal transcribed spacer II (ITS2) sequences. Bayesian posterior probability values are shown. Only probabilities greater than 0.5 (>0.5) are indicated above the branches. The species names based on morphological identification are to the right of the voucher code (**Table 1**). Candidate species were numbered in ascending order after the name of their closest species. *Brevipalpus* species groupings are highlighted in colored squares: blue = Clade I; purple = Clade II, hitherto with a single representative species (*B. n. sp.* from Argentina); rose = Clade III; yellow = Clade IV; green = Clade V and light rose = Clade VI. *Cenopalpus pulcher* and *Raoiella* sp. (*R. indica* and *R. macfarlanei*) were used as sisters and outgroups, respectively.



508
509
510
511
512
513
514
515
516

Figure 2. Bayesian phylogeny constructed using sequence data obtained from the concatenated dataset consisting of: A. mitochondrial fragments (*COI* barcoding region and *COI* DNF–DNR); B. nuclear fragments (subunit D1–D3 28S and ITS2). Statistical supports indicate the Bayesian posterior probability values. Only probabilities greater than 0.5 (>0.5) are indicated above the branches. The species names based on morphological identification are to the right of the voucher code (Table 1). Candidate species were numbered in ascending order after the name of the closest species. Putative *Brevipalpus* species groupings are highlighted in colored squares: blue = Clade I; purple = Clade II, hitherto with a single representative species (*B. n. sp.* from Argentina); rose = Clade III; yellow = Clade IV; green = Clade V and light rose = Clade VI. *Cenopalpus pulcher* and *Raoiella* spp. (*R. indica* and *R. macfarlanei*) were used as sisters and outgroups, respectively.

517 **Table 2.** Sets of DNA sequences of *Brevipalpus* species and putative species supported by phylogeny
 518 for each DNA fragment studied. Gray blocks indicate taxa with nonamplified DNA sequences for the
 519 respective fragments.

Clade	COI barcode	COI DNF-DNF	subunit D1-D3	ITS2
Clade I	<i>B. yothersi</i>	<i>B. yothersi</i>	<i>B. yothersi</i>	<i>B. yothersi</i>
	<i>B. near yothersi</i> 1	<i>B. near yothersi</i> 1	<i>B. near yothersi</i> 1	-
	<i>B. near yothersi</i> 2	<i>B. near yothersi</i> 2	<i>B. near yothersi</i> 2	<i>B. near yothersi</i> 2
	<i>B. incognitus</i>	<i>B. incognitus</i>	<i>B. incognitus</i>	<i>B. incognitus</i>
	<i>B. near incognitus</i> 1	-	<i>B. near incognitus</i> 1	<i>B. near incognitus</i> 1
	<i>B. near incognitus</i> 2	<i>B. near incognitus</i> 2	<i>B. near incognitus</i> 2	<i>B. near incognitus</i> 2
Clade II	<i>B. new sp.</i>	<i>B. new sp.</i>	<i>B. new sp.</i>	<i>B. new sp.</i>
Clade III	<i>B. californicus</i> s.s.	<i>B. californicus</i> s.s.	<i>B. californicus</i> s.s.	<i>B. californicus</i> s.s.
	<i>B. near californicus</i> 1	<i>B. near californicus</i> 1	-	-
	-	<i>B. near californicus</i> 2	-	-
	<i>B. lewisi</i>	<i>B. lewisi</i>	<i>B. lewisi</i>	<i>B. lewisi</i>
Clade IV	<i>B. phoenicis</i>	<i>B. phoenicis</i>	<i>B. phoenicis</i>	<i>B. phoenicis</i>
	<i>B. papayensis</i>	<i>B. papayensis</i>	<i>B. papayensis</i>	<i>B. papayensis</i>
	<i>B. ferraguti</i>	<i>B. ferraguti</i>	<i>B. ferraguti</i>	<i>B. ferraguti</i>
	<i>B. obovatus</i>	<i>B. obovatus</i>	<i>B. obovatus</i>	<i>B. obovatus</i>
	<i>B. chilensis</i>	<i>B. chilensis</i>	<i>B. chilensis</i>	<i>B. chilensis</i>
Clade V	<i>B. mallorquensis</i>	<i>B. mallorquensis</i>	<i>B. mallorquensis</i>	<i>B. mallorquensis</i>
	-	<i>B. near mallorquensis</i>	-	<i>B. near mallorquensis</i>
Clade VI	<i>B. oleae</i> .	<i>B. oleae</i> .	<i>B. oleae</i> .	-

520 **Genetic distance-based analysis**

521 **Species hypothesis using intra- and intergenetic distances**

522 Distance values for overall sequence pairs for each genome fragment, as well as exclusively
 523 for sequences of *Brevipalpus* species (K2P and *p*-distance), are summarized in **Table 3**. The mean
 524 intraspecific variability of the studied *Brevipalpus* species/putative species is also presented. The
 525 highest mean variabilities were recorded in the mitochondrial COI barcoding and the nuclear ITS2.
 526 Single matrices of distances of pairwise comparisons between–and within–*Brevipalpus*
 527 species/putative species for all fragments are presented in **Tables SM2-11–SM2-18**.

528 **Table 3.** Mean overall interspecific divergence for the sequence pairs and for sequences of *Brevipalpus*
 529 species, minimum and maximum divergence, and the standard error (SE). The mean intraspecific
 530 variability (minimum and maximum) observed in *Brevipalpus* species. Values indicate Kimura 2
 531 parameters and *p*-distance.

Genomic region	Interspecific divergence				Intraspecific divergence	
	K2P distance		<i>P</i> -distance		<i>Brevipalpus</i>	
	Mean (%)	range (%) (S.E.%)	Mean (%)	range (%) (S.E.%)	Mean (%) (min.-max.%)	
	All sequences	<i>Brevipalpus</i> sequences	All sequences	<i>Brevipalpus</i> sequences	K2P dist.	<i>p</i> -distance
COI barcoding	11.31 (0.0-27.7) (1.56)	9.86 (0.0-21.86) (1.44)	10.28 (0.0-23.09) (1.29)	9.11 (0.0-18.95) (1.22)	1.12 (0.0-2.44)	1.11 (0.0-2.40)
COI DNF-DNF	5.55 (0.0-21.78) (1.09)	5.45 (0.0-18.77) (1.19)	5.23 (0.0-18.87) (1.10)	5.14 (0.0-16.60) (1.09)	0.91 (0.0-4.28)	0.79 (0.0-4.15)
D1-D3	7.13 (0.0-33.41) (1.1)	6.65 (0.0-22.70) (1.06)	6.48 (0.0-26.45) (0.95)	6.11 (0.0-19.24) (0.93)	1.90 (0.0-2.86)	1.87 (0.2-2.81)
ITS2	12.11 (0.0-93.52) (2.32)	11.00 (0.0-42.02) (2.19)	10.42 (0.0-52.07) (1.75)	9.79 (0.0-31.80) (1.72)	4.83 (0.0-13.07)	4.60 (0.0-11.98)

532

533

534 According to the *COI* barcoding region, the lowest interspecific genetic divergences were
535 recorded between: i) *B. chilensis* and *B. ferraguti* (\bar{X} distance = 3.11%, ranging from 2.64% to
536 3.49%); and ii) *B. obovatus* and *B. chilensis* (\bar{X} = 3.27%, 2.83–3.70%) (Tables SM2-11–SM2-18).
537 These species were recognized as trusty closely related taxa (Navia *et al.* 2013). These reference
538 values suggest that *B. near yothersi* 1 and *B. n. yothersi* 2 represent a taxon distinct from *B.*
539 *yothersi* (\bar{X} = 3.75% and 3.81% distances, respectively); however, these two putative taxa could
540 not be discriminated from each other (\bar{X} = 2.18%, 1.96%–2.40%) because the genetic divergence
541 values were lower than those in the references. The same pattern was observed for *B. n.*
542 *incognitus* 1 and *B. n. incognitus* 2, *i.e.*, these putative taxa can be regarded as different from *B.*
543 *incognitus* (\bar{X} = 7.66 and 7.44% distances, respectively), but the reference values did not support
544 the partition between them (\bar{X} = 1.99%). The *COI* barcoding region robustly discriminated *B. n.*
545 *californicus* 1 and *B. californicus* s.s. (\bar{X} = 4.58%), indicating that they are two different species.

546 The *COI* DNF–DNR distance values were lower overall than those observed for the barcoding
547 fragment. The lowest interspecific genetic divergence for the *COI* DNF–DNR fragment was
548 observed between *B. chilensis* and *B. obovatus* (\bar{X} = 3.25%, 1.91%–4.70%), similar to that
549 observed in the *COI* barcoding region. This value indicates that the putative species *B. n.*
550 *incognitus* 2 is differentiated from *B. incognitus* by a large distance (\bar{X} = 6.59%, 5.90–7.14 %).
551 *Brevipalpus californicus* s.s. was kept apart from *B. near californicus* 1 (\bar{X} = 3.57%, 3.48%–4.29%)
552 and from *B. near californicus* 2 (\bar{X} = 2.70%, 2.70%–2.70%). The distance between *B. near*
553 *californicus* 1 and *B. n. californicus* 2 (\bar{X} = 2.37%, 2.3–3.08%) was not enough to discriminate
554 them. *Brevipalpus mallorquensis* was differentiated from *B. n. mallorquensis* (\bar{X} = 3.69%, 3.49–
555 3.89%) (Tables SM2-11–SM2-18).

556 The lowest D1–D3 interspecific distance was recorded between *B. yothersi* and *B. incognitus*
557 (\bar{X} = 0.68%, 0.40%–1.01%) and between *B. phoenicis* s.s. and *B. papayensis* (\bar{X} = 1.52%, 1.21–
558 1.83%) (Tables SM2-11–SM2-18). Based on these lowest reference values, the putative species
559 *B. n. incognitus* 1 could be separated from *B. n. incognitus* 2 (\bar{X} = 1.77%, 0.81%–3.49%). These
560 two putative species also showed distance values that clearly distinguished them from *B.*
561 *incognitus*–*B. incognitus* x *B. n. incognitus* 1 (\bar{X} = 1.6%, 0.40%–3.49%) and *B. incognitus* x *B. n.*
562 *incognitus* 2 (\bar{X} = 1.18%, 1.011–1.21%). According to these reference values, *B. yothersi* could not
563 be differentiated from its related putative species and not even *B. n. yothersi* 1 x *B. n. yothersi* 2.
564 All other putative species could be discriminated by D1–D3 distances.

565 For the nuclear ITS2 fragment, *B. californicus* ss. and *B. lewisi* exhibited the lowest interspecific
566 distance (\bar{X} distance = 0.93%, 0.93%–1.40%). All the putative species delimited by morphology
567 and phylogeny, *i.e.*, *B. n. yothersi* 2, *B. n. incognitus* 1, *B. n. incognitus* 2, and *B. n. mallorquensis*,
568 could be discriminated by the output values of the ITS2 distances.

569 **ABGD-Automatic Barcode Gap Discovery for species-delimitation method**

570 The ABDG results, including relative gap width (X), prior intraspecific distance (P), prior
571 maximal distances (PMD), and barcode gap distance (BGD) computed by the K2P and p -distance
572 model algorithms, are shown in Table 4. The number of candidate species was consistent whether
573 analyzing the total set of sequences or when separated by clades, therefore, only the results from
574 the total set were discussed.

575 Analysis of the *COI* barcoding dataset using the K2P distance model recovered 20–21
576 Molecular Operational Taxonomic Units (MOTU's, Floyd *et al.* 2002) (Table 4). The 17 species
577 identified through phylogeny/morphology and three additional taxa within the *B. chilensis* taxon—
578 specimens from *Ribes punctatum* (MG458824), *Magnolia grandiflora* (MG458832), and *Ligustrum*
579 *sinense* (MG458834) - were recognized across various relative gap widths (X = 1.0, 1.25, and 1.5).
580 Notably, Clade I exhibited variation in taxa composition at X = 1.0 and X = 1.25 relative gap widths,
581 resulting in 21 MOTUs. Specifically, at X = 1.0, sequences of *B. yothersi* from *Cecropia*
582 *pachystachya* (MG458858) were identified as a potential distinct species. Interestingly, at X = 1.25,
583 specimens from *C. pachystachya* clustered within *B. yothersi*, whereas *B. n. yothersi* 2 from

584 *Delonix regia* (MG458843, MG458845) formed a separate lineage from other specimens of *Citrus*
585 sp. (MG458827, MG458830) within *B. near yothersi* 2. At X = 1.5, 20 MOTUs were identified, and
586 no isolated species were detected within *B. yothersi* and *B. near yothersi* 2. The *p*-distance
587 algorithm applied to the *COI* dataset returned fewer MOTUs. The putative species within *B.*
588 *chilensis* did not emerge when this algorithm was used, and 18 MOTUs were identified. When X =
589 1.0 and X = 1.25 were used, 17 species consistent with the phylogeny/morphology and one
590 putative species were identified. Notably, at X = 1.0, *B. near yothersi* 2 from *D. regia* (MG458843,
591 MG458845) was identified as a distinct candidate species separated from those of *B. near yothersi*
592 2 from *Citrus* sp. (MG458827, MG458830). Similar results were observed when the K2P distance
593 was applied at X = 1.25. In contrast, at X = 1.25, specimens from *D. regia* and *Citrus* sp. grouped
594 together as *B. near yothersi* 2, whereas *B. yothersi* from *C. pachystachya* (MG458858) remained
595 separate, no partitions were observed at X = 1.5.

596 **Table 4.** Number of candidate species revealed ABGD analysis of *Brevipalpus* sequences per fragment
597 (*COI* DNA barcoding, *COI* DNF–DNR, subunit D1–D3, and ITS2 region) estimated by *p*-distance and
598 Kimura-2-parameters substitution model algorithms

Genome region	Model Algorithm	X	Nb of species	PID	PMD	BGD
COI barcoding	K2P distance	1.00	21	0.001	0.0046	0.016
		1.25			0.0077	0.058
		1.50			0.0046	0.058
	<i>p</i> -distance *	1.00	18	0.001	0.001	0.027
		1.25	18			0.051
		1.50				
COI DNF–DNR	K2P distance	1.00	20	0.00278	0.00774	0.016
		1.25				
		1.50				
	<i>p</i> -distance *	1.00	20	0.001	0.0046	0.018
		1.25				
		1.50				
D1–D3 subunit	K2P distance	1.00	19	0.00167	0.00167	0.006
		1.25				
		1.50				
	<i>p</i> -distance	1.00	20	0.001	0.001	0.006
		1.25				
		1.50				
ITS2 region	<i>p</i> -distance	1.5	18	0.001	0.001	0.042
		1.00				
		1.25	17	0.001	0.001	0.047
		1.50				

599 X = relative gap width. Nb species = number of candidate species. PID = prior intraspecific distance, partition using
600 a range of 0.001 (P_{\min}) to 0.1 (P_{\max}) (0.001, 0.001668, 0.002783, 0.004642, 0.007743, 0.012915, 0.021544,
601 0.035938, 0.059948, 0.1000). PMD = prior maximal distances. BGD = barcode gap distance. * X = 1.0, 1.25 or 1.5
602 means that no partition was observed.

603 The **COI DNF–DNR** sequences analyzed by the **K2P** distance (X = 1.0, 1.25, and 1.5) revealed
604 20 MOTUs. This number of MOTUs matched the 18 species/putative species shown by phylogeny
605 along with two candidate species: *B. papayensis* from *Citrus* sp. (DQ450486, DQ450485) and *B.*
606 *obovatus* from *Cestrum nocturnum* (KC291386), both from Brazil. The latter specimens were
607 sequenced only for this fragment. Using the **p-distance** model (X = 1) the same main species
608 previously described for the K2P were recovered. However, for X = 1.25 and 1.5, the analyses
609 resulted in an inaccurate assessment of the species with many partitions emerging as 29 putative
610 species. This structure does not correspond to the scenario that arises from our studies based on
611 conventional taxonomy.

612 Analysis of the subunit **D1-D3** sequences using the **K2P** model and the three values of relative
613 gap width ($X = 1.0, 1.25, \text{ and } 1.5$) revealed 19 MOTUs (**Table 4**), three more than those detected
614 by phylogenetic analysis (16 MOTUs; **Table 2**). The distribution of sequences differed from that
615 observed for the mitochondrial markers. For example, *Brevipalpus yothersi*, *B. near yothersi 1*, and
616 *B. near yothersi 2* were grouped into a single Clade. Another difference was observed within *B.*
617 *incognitus* and its putative species: two sequences of *B. incognitus* from *Cocus nucifera*
618 (MK293652 - MK293653) in Brazil stayed apart as a new putative taxon separate from the other
619 comprising *B. incognitus*, *B. near incognitus 1*, and *B. near incognitus 2*. *Brevipalpus obovatus*
620 was assigned into three candidate lineages depending on to the origin of its host plants, *i.e.*,
621 populations from *Coniza bonariensis* (MK293694- MK293697) and *Helichrysum stoechas*
622 (MK293700 - MK293701), from Spain, and *Solanum violifolium* (MK293698 MK293699) from
623 Brazil. In Brazil, the sequence KP276421 of *B. papayensis* (unknown host plant) was sequenced
624 only for this fragment and was separated from *B. papayensis* (MT664799-MT664800), which was
625 found on *Coffea* sp. leaves. Additionally, *Brevipalpus chilensis* (Chile) from *Magnolia grandiflora*
626 (MK293716; MK293671) was distinct from specimens collected from *Ribes punctatum*
627 (MK293643-MK293646; MK29371-MK293715). One more MOTU (20) was identified by the *p*-
628 distance ($X = 1.0, 1.25, \text{ and } 1.5$), with clusters similar to those observed for K2P, except for
629 *Brevipalpus n. yothersi 2* from *D. regia* (MK293681; K293683), which was separate from
630 *Brevipalpus yothersi*, *B. near yothersi 1*, and *B. near yothersi 2* from *Citrus* sp. suggesting a new
631 candidate species.

632 Eighteen MOTUs were recovered by applying the K2P ($X = 1.25, 1.5$) for ITS2 sequences, in
633 contrast to the 15 taxa recovered by phylogeny. *Brevipalpus yothersi* and its putative species (*B.*
634 *near yothersi 2*) grouped with *B. near incognitus 1*, whereas *B. incognitus* and *B. near incognitus*
635 *2* stayed apart. There were no ITS2 sequences obtained for the *B. n. yothersi 1* specimen (**Table**
636 **2**). The partitions of the three following species differed according to the host plant or geographical
637 region. *Brevipalpus papayensis* has been split into two different lineages according to the host
638 plant (*Ligustrum. sinense*, MH818180-MH818186 and *Coffea* sp., MT660805-MT660806). A
639 similar partition pattern was recorded for *B. obovatus*, which had three lineages- *C. bonariensis*
640 (MH818198-MH818201), *H. stoechas* (MH818195-MH8181957) from Spain, and *L. sinense* from
641 Brazil (MH818177-MH818179), and *B. chilensis* with three lineages- *M. grandiflora* (MH818206),
642 *R. punctatum*, (MH818127 and MH818205), and *L. sinense* (MH818139-MH818142). The smallest
643 relative gap width ($X = 1.0$) resulted in 66 putative species; hence it was disregarded. The *p*-
644 distance model recovered 17 MOTUs's ($X = 1.0, 1.25, 1.5$). Here, *B. incognitus* clustered with *B.*
645 *yothersi*, *B. near yothersi 2*, and *B. near incognitus 1*. Only *B. near incognitus 2* stayed apart in
646 Clade I; all 16 remaining taxa split as shown by K2P.

647 **ASAP-Assemble Species by Automatic Partitioning tool**

648 ASAP results are summarized in **Table 5** and **Figure SM1-8**. Using an adequate ASAP-score
649 (5.5) and a high probability ($1.89e-02$), the *COI* barcoding sequences, processed by the K2P
650 method, split into 17 taxa, consisting of 11 species and six candidate species, keeping the same
651 structure recovered by morphological taxonomy (**Figure SM1-8**). The *COI* barcoding dataset
652 calculated by the *p*-distance method revealed 16 MOTUs, as *B. near incognitus 1* and *B. near*
653 *incognitus 2* were recognized as a single group.

654 Analysis of *COI* DNF-DNR, subunit D1-D3, and region ITS using the ASAP method produced
655 similar results both under the K2P and *p*-distance models. Therefore, only the results obtained
656 under the K2P model are described further. The *COI* DNF-DNR sequences returned 20 taxa,
657 including 11 species, 7 putative species, and 2 extra new candidates: *B. papayensis* from *Citrus*
658 sp. (DQ450485-DQ450486) and *B. obovatus* from *Cestrum nocturnum* (KC291386), in Brazil. The
659 ABGD method confirmed this pattern. The latter sequences (DQ450485/DQ450486 and
660 KC291386) were unique to the *COI* DNF-DNR fragment.

661 Fifteen species were detected by ASAP for sequences of the subunit D1-D3. *Brevipalpus near*
662 *yothersi 1* and *2* were clustered together with *B. yothersi* in a single taxon. Likewise, *B. near*
663 *incognitus 1* was also grouped with *B. incognitus*. *Brevipalpus n. incognitus 2* remained isolated.
664 Additionally, three candidate species were assigned to the *B. obovatus* taxon namely, *B. obovatus*

665 from *C. bonariensis* (MK293695-MK293697), *H. stoechas* (MK293700-MK293701) from Spain,
 666 and *S. violifolium* (MK293698- MK293699) from Brazil. This structure was revealed under the best
 667 score suggested by ASAP (score = 11.50, p -value = 6.61e-01).

668 **Table 5.** Number of *Brevipalpus* species (K2P method) predicted with the best Assemble Species by
 669 Automatic Partitioning (ASAP)-score based on mitochondrial (*COI* DNA barcode and *COI* DNF–DNR)
 670 and nuclear (subunit D1–D3 and ITS2) sequences.

Genome region	Nb of species	Partition	ASAP score	P -val (rank)	W (rank)	Threshold Dist. (D_t)	inter/intra	Distance (D_c)
COI barcoding	17	3.00	5.5	1.89e-02	2.87e-04	0.018560	2.87e-04	0.018587
COI DNF-DNR	20	10.00	15.00	6.43e-01	4.94e-06	0.015320	0.016690	4.94e-06
D1-D3 subunit	15	7.00	11.50	6.61e-01	3.39e-05	0.008658	3.39e-05	0.009759
ITS2 region	17	3.00	7.50	2.69e-01	9.32e-05	0.029646	9.32e-05	0.33167

671
 672 W = relative gap width; p -value = probability of merging the groups within the node of the ultrametric hierarchical
 673 clustering tree; D_t = threshold distance to which this node corresponds (jumping distance); inter/intra = threshold
 674 between intra- and interspecific distance; D_c = current clustering distance (grouping distance).

675 The ITS2 sequences revealed a structure with 17 MOTUs. Similar to the subunit D1–D3, a
 676 single taxon was recovered for *B. yothersi* and *B. near yothersi* 2. *Brevipalpus incognitus* and its
 677 putative species remained separate. *Brevipalpus papayensis* lineages from *L. sinense*
 678 (MH818180- MH818186) were distinct from those collected from *Coffea* sp. (MT664805-
 679 MT664806). Likewise, *B. obovatus* lineages from *C. bonariensis*/*H. stoechas* in Spain (MH818195-
 680 MH818197/MH818198- MH818201) have been separated from *L. sinense* in Brazil (MH818177-
 681 MH818179). *Brevipalpus chilensis* was assigned into three candidate lineages, *i.e.*, populations
 682 collected on *M. grandiflora* (MH818206), *R. punctatum* (MH818127 and MH818205), and *L.*
 683 *sinense* (MH818139- MH818142) (**Figure 2B**).

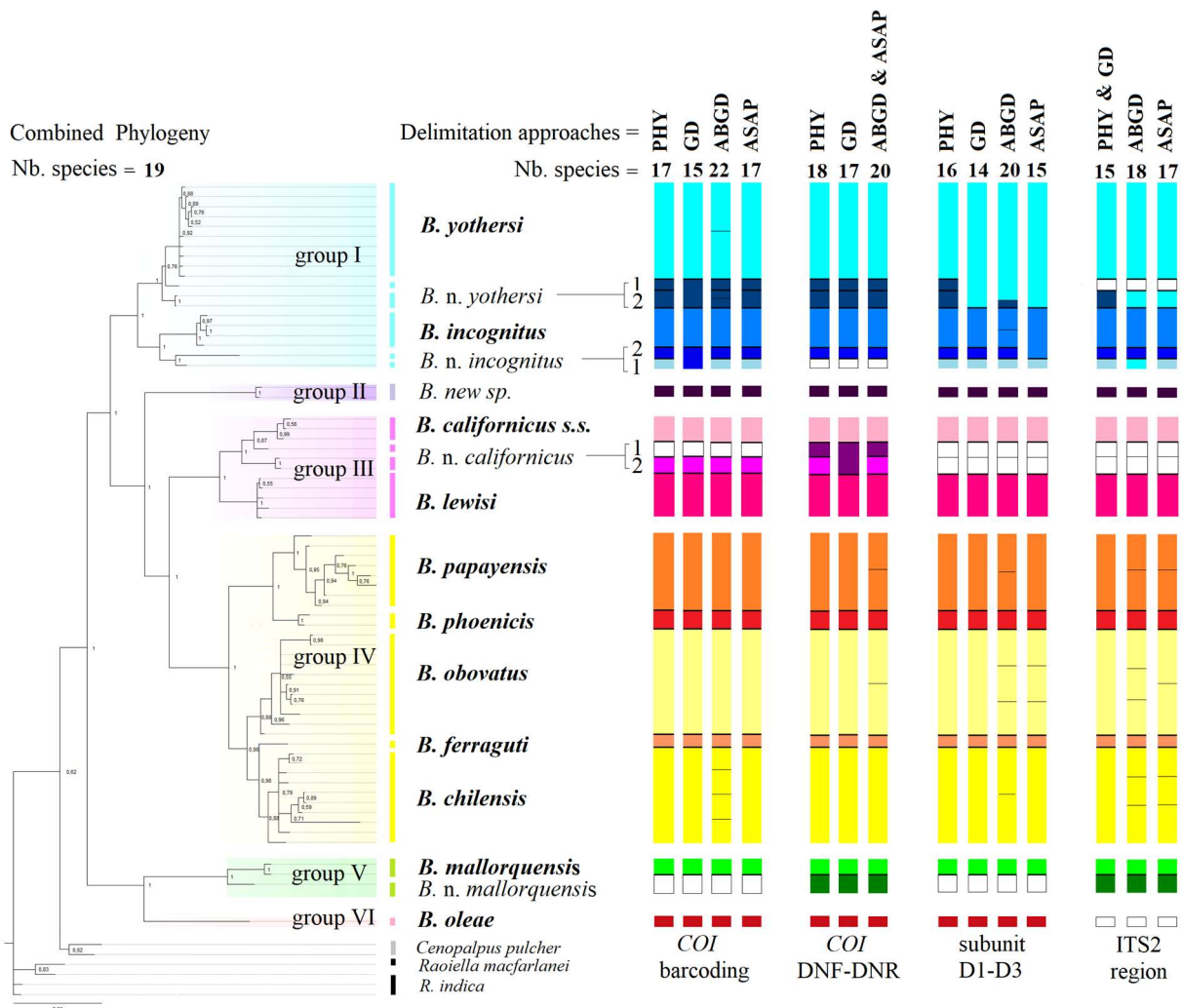
684 Exploring the species-delimitation methods and molecular markers

685 The findings confirmed the presence of a new species in Clade II (*B. new sp.*) and the status
 686 of Clade VI (*B. oleae*) through consistent and well-supported hypotheses, achieved by
 687 morphology, phylogenetic inferences, and distance delimitation methods (**Figure 3**). Putative
 688 species in Clades III and V, *B. n. californicus* 1, *B. n. californicus* 2, and *B. n. mallorquensis*, were
 689 also supported by phylogeny and by all species-delimitation methods. However, ambiguities were
 690 observed for some taxa in Clades I and IV (**Figure 3**).

691 In Clade I, a distinct lineage of *B. n. yothersi* 2 from *Delonix regia* (Piracicaba, BR) was
 692 identified, separate from the *B. n. yothersi* 2 collected from *Citrus* sp. (Argentina) based on *COI*
 693 fragments, whereas the results for the nuclear fragments were quite variable. Similarly, *B. yothersi*
 694 from *Cecropia pachystachya* was regarded as an isolated lineage only by the *COI* barcode
 695 fragment. Unlike mitochondrial markers, the nuclear markers did not detect enough nucleotide
 696 divergence to distinguish all the putative species in Clade I. In Clade IV, potential cryptic species
 697 were identified within *B. papayensis*, *B. obovatus*, and *B. chilensis*, with distinct associations with
 698 specific host plants (**Table SM2-19; Figure 3**) and with consistent results across both molecular
 699 markers and methods. *Brevipalpus papayensis* from *Citrus* sp. (*COI* fragment) and from *Coffea* sp.
 700 (nuclear fragments) were separated from specimens collected from other hosts. Additionally, *B.*
 701 *obovatus* from *C. bonariensis*, *H. stoechas* and *S. violifolium* and *B. chilensis* from *M. grandiflora*,
 702 *R. punctatum*, and *L. sinense* (**Table SM2-19**) were separated by the ABGD and ASAP
 703 approaches based on mitochondrial and nuclear markers (**Figure 3; SM2-19**).

704
 705

706



709 **Figure 3.** Bayesian inference tree showing the phylogenetic relationships among *Brevipalpus* lineages
 710 based on concatenated datasets (COI barcoding, COI DNF-DNR, subunit D1–D3, and ITS2). Differently
 711 colored clades represent species groups, with bars of the same color tones on the right indicating the
 712 number of species (bold) and putative species (regular) according to phylogeny (PHY), genetic distance
 713 (GD), and delimitation approaches ABGD and ASAP using K2P and *p*-distance models, various
 714 partitions, and relative gap width values ($X = 1.0, 1.25, 1.5$). White samples are not available. Bayesian
 715 posterior probability (BPP) values ≥ 0.98 were considered to indicate well-supported putative
 716 species.

717 The ABGD results were dependent on the chosen model (Kimura and *p*-distance) and were
 718 also affected by changes in the gap width parameter. Applying the standard settings ($X = 1.5$), no
 719 barcode gap was observed, and only one partition was detected for the mitochondrial fragments.
 720 When lowering the *X*-value (1.0 X -1.25), the COI sequences were clustered into different entities,
 721 which was more congruent with the phylogeny and morphology findings. Similar results were
 722 observed by Jörger *et al.* (2012). Species recovered based on the COI DNF-DNR dataset were
 723 only distinguished when a smaller relative gap width ($X = 1$) was used, as larger values (1.25 and
 724 1.5) grouped all sequences together. Therefore, for analyzing the COI DNF-DNR, an $X = 1$ was
 725 sufficient to detect potential partitions among the *Brevipalpus* populations. Similarly, smaller
 726 relative gaps in the COI barcode dataset revealed distinct species, whereas larger gaps grouped
 727 all sequences into a single taxon. The k2P model yielded more entities than the *p*-distance models
 728 across various gap widths, except for the nuclear marker D-D3. The barcoding gaps tend to be
 729 larger under the K2P model than with uncorrected *p*-distance models (Srivathsan & Meier, 2012).

730 For sequences with small interspecific distances (<5%) from closely related species, *p*-distances
 731 were deemed more suitable than K2P (Nei & Kumar, 2000). Previous studies have shown that
 732 using *p*-distances could result in higher or similar identification success rates than K2P correction
 733 (Srivathsan & Meier, 2012).
 734

735 ***Brevipalpus* species: Intra- and interspecific thresholds based on polynomial regression**
 736 **fitting**

737 Threshold values of the genetic distance (GD) for demarcation of *Brevipalpus* species were
 738 calculated for each region of the genome, and the results are summarized in **Table 6** (see **Figure**
 739 **SM1-9**). The maximum value of the confidence interval, CI-Max, represents the highest point of
 740 the polygon (CI-max = 3.95%); higher values (>CI-Max) observed between two taxa support that
 741 they are different species. The magnitude and extent of the distance values varied according to
 742 the fragment analyzed. The subunit D1–D3 variation values were lower than those observed for
 743 the mitochondrial regions, with $y = 1.76\%$ (0.7-2.82%) and $\alpha = 2.04\%$. For the ITS2 region, values
 744 extending upward were registered and $y = 7.75\%$ (CI = 4.37-11.14%) and $\alpha = 6.53\%$ (**Table 6**).
 745 The amplitude of the confidence interval was higher for the ITS2 fragment (6.77) and for the COI
 746 DNF–DNR (4.42).
 747

748 **Table 6.** Number of sequences and pairwise distance comparisons for COI barcoding, COI DNF–DNR,
 749 subunit D1–D3, and ITS2 sequences of *Brevipalpus* species using the *p*-distance model. Values were
 750 calculated using a polynomial regression fitting curve with a confidence interval of 95%.

Genome region	Number of sequences	number of pairwise comparisons	Number of inter difference values	Intersection point (y)	Confidence intervals (CI) (%)	highest intraspecific vs. lowest interspecific (α) (%)
COI barcoding region	79	3,487	136	2.54%	1.14–3.95	3.27
COI DNF-DNR	427	91,807	153	3.34%	1.31–5.73	3.23
D1–D3	96	4,657	121	1.76%	0.7–2.82	2.04
ITS2	117	6,787	153	7.75%	4.37–11.14	6.53

751 **DISCUSSION**

752 **Species-group rearrangements and informative morphological traits**

753 The multiloci and integrative approach adopted in this study allowed for substantial advances
 754 in species-group rearrangements as well as species-delimitation criteria. Although only 11 valid
 755 species were evaluated in this study out of the 292 valid species (Castro et al., 2024), the analysis
 756 included taxa representing four of the six species groups established by Baker & Tuttle (1987) and
 757 all species of major agricultural importance (Hebert et al., 2003; Childers & Rodrigues, 2011; Beard
 758 et al., 2015). Results showed that the current division of *Brevipalpus* into species groups only
 759 partially corresponded to phylogenetic branches; therefore, a rearrangement of species groups is
 760 proposed (**Table 7**). The findings allow a discussion on phylogenetically informative morphological
 761 traits and a review of the definition of each species group.

762 **Table 7** summarizes the morphological characters used to separate the currently accepted six
 763 species groups according to Baker & Tuttle (1987) and highlights the discrepancies between these
 764 criteria and the molecular analyses herein obtained. The phylogenetic study has uncovered the
 765 following inconsistencies: (i) species previously classified as part of the *phoenicis* species group,
 766 including *B. yothersi*, *B. incognitus*, *B. phoenicis*, *B. papayensis*, and *B. ferraguti*, are polyphyletic
 767 and are set into two distinct clades (Clades I and IV). Remarkably, *B. yothersi* and *B. papayensis*,

768 two former synonyms of *B. phoenicis* resurrected by Beard *et al.* (2015), have been placed in two
 769 different clades. Additionally, *B. phoenicis*, the exemplar species of the *phoenicis* group, was
 770 clustered together with *B. obovatus*, the exemplar species of the *obovatus* group, in Clade IV; (ii)
 771 *Brevipalpus lewisi* and *B. oleae* considered to be part of the *cuneatus* species group, along with
 772 two potential species displaying morphological traits of the *cuneatus* species group, were also
 773 found to be polyphyletic and were split into three clades (Clades III, V, and VI). *Brevipalpus lewisi*
 774 was clustered with *B. californicus* ss, the exemplar species of the *californicus* group, in Clade III.
 775 *Brevipalpus oleae* formed a separate Clade (Clade VI) distinct from *B. mallorquensis* and *B. n.*
 776 *mallorquensis* (Clade V), as previously noted by Alves *et al.* (2019). Interestingly, the new
 777 specimens from *Citrus*, Argentina (MG458828/29; MH204695/96; MK293669/70; MH818133/34)
 778 were separated as a different lineage, although following Baker and Tuttle they should be placed
 779 in the *obovatus* group.

780 **Table 7.** Arrangement of *Brevipalpus* taxa according to the molecular-based clades, main
 781 morphological traits, and their membership in the species-group established by Baker & Tuttle (1987).

Clade	species & putative species	Morphological traits				Baker & Tuttle (1987) (BP)	
		DLO setae	f2	T2 sol.	Palp seg palp setae		
I	<i>B. yothersi</i>	6	0	2	4	3	<i>phoenicis</i>
	<i>B. near yothersi</i> 1	6	0	2	4	3	<i>phoenicis</i>
	<i>B. near yothersi</i> 2	6	0	2	4	3	<i>phoenicis</i>
	<i>B. incognitus</i>	6	0	2	4	3	<i>phoenicis</i>
	<i>B. near incognitus</i>	6	0	2	4	3	<i>phoenicis</i>
II	<i>B. n. sp. Argentina</i>	6	0	1	4	3	<i>obovatus</i>
III	<i>B. californicus</i>	7	1	2	4	3	<i>californicus</i>
	<i>B. near californicus</i> 1	7	1	2	4	3	<i>californicus</i>
	<i>B. near californicus</i> 2	7	1	2	4	3	<i>californicus</i>
	<i>B. lewisi</i>	7	1	1	4	3	<i>cuneatus</i>
IV	<i>B. chilensis</i>	6	0	1	4	3	<i>obovatus</i>
	<i>B. obovatus</i>	6	0	1	4	3	<i>obovatus</i>
	<i>B. ferraguti</i>	6	0	2	4	3	<i>phoenicis</i>
	<i>B. papayensis</i>	6	0	2	4	3	<i>phoenicis</i>
	<i>B. phoenicis</i>	6	0	2	4	3	<i>phoenicis</i>
V	<i>B. mallorquensis</i>	7	1	1	4	3	<i>cuneatus</i>
	<i>B. near mallorquensis</i>	7	1	1	4	3	<i>cuneatus</i>
VI	<i>B. oleae</i>	7	1	1	4	3	<i>cuneatus</i>

782 **DLO setae** = number of dorsolateral setae on opisthosoma; **f2** = dorsal setae (presence = 1 or absence = 0); **T2**
 783 **sol.** = number of solenidia at the apex of tarsus II of the female; **palp seg.** = number of papal segments; **palp**
 784 **setae** = number of setae on the apical segment of the palpus; **BP** = groups following Baker & Tuttle 1987 indicating
 785 where the species in this study would be classified if following Baker & Tuttle (1987) classification.

786 Considering these inconsistencies, a new species-group rearrangement is proposed. To avoid
 787 confusion with all the previous *Brevipalpus* classifications (Baker *et al.*, 1975; Meyer, 1979; Baker
 788 & Tuttle, 1987), in which specific names were used to designate species groups, the Roman
 789 numeral nomenclature is adopted. As the taxonomic knowledge of the genus evolves and new
 790 genetic lineages are detected, they may be assigned subsequent Roman numerals. Hence, the
 791 proposed composition of the six *Brevipalpus* species groups is as follows: I) *B. yothersi* and *B.*
 792 *incognitus*; II) *B. new sp.* collected from citrus in Argentina; III) *B. californicus* and *B. lewisi*; IV) *B.*
 793 *papayensis*, *B. phoenicis*, *B. obovatus*, *B. ferraguti*, and *B. chilensis*; V) *B. mallorquensis* collected
 794 from *Rosmarinus officinalis*, and a near species from *Helichrysum stoechas* from Spain, and VI)
 795 *B. oleae* (**Table 7**). Additionally, the cryptic species detected in this study will be members of
 796 *Brevipalpus* species groups I, III and V. Although some of the proposed species groups are
 797 currently composed of only one species, as new taxa are characterized and included in the
 798 phylogeny, they may be grouped with these species.

799 Incongruences between the phylogenetic groups and the Baker & Tuttle classification indicate
800 that some of the accepted taxonomic criteria are inappropriate for building a higher species-level
801 classification. Species clustered in the same Clade share the same state for some of these
802 characters but not for others. The number of dorsolateral setae on the opisthosoma was consistent
803 among species of the same Clade (**Tables 7; SM2-20**) and, according to current knowledge, could
804 be useful as a species-group diagnostic character. However, distantly related clades, e.g., III and
805 V/VI, shared the presence of the seta *f2* totaling seven dorsolateral setae, suggesting that this trait
806 arose independently in separate lineages in the genus and would not be phylogenetically
807 informative. In contrast, the number of solenidia on tarsus II varied among species in clades III and
808 IV (**Table 7; SM2-20**), indicating that this feature should not be used for division of the genus.

809 Unfortunately, from the analyzed dataset, it was impossible to evaluate the phylogenetic value
810 of the number of palpal segments and the number of setae on the distal segment of the palps.
811 These traits were used to delimit the *portalis* and *frankeniae* species groups and were not variable
812 among the studied species. Discrepancies in the morphology of the *portalis* species group have
813 already been pointed out by Alves *et al.* (2019). A species morphologically very similar to *B.*
814 *cuneatus*, *Brevipalpus sulcatus* Alves, Ferragut & Navia, was classified as belonging to the *portalis*
815 species group (Alves *et al.*, 2019). A better understanding of the phylogenetic relevance of these
816 characters depends on the integration of species with variable traits in the *Brevipalpus* phylogeny,
817 including those previously classified as belonging to the *portalis* and *frankeniae* groups.

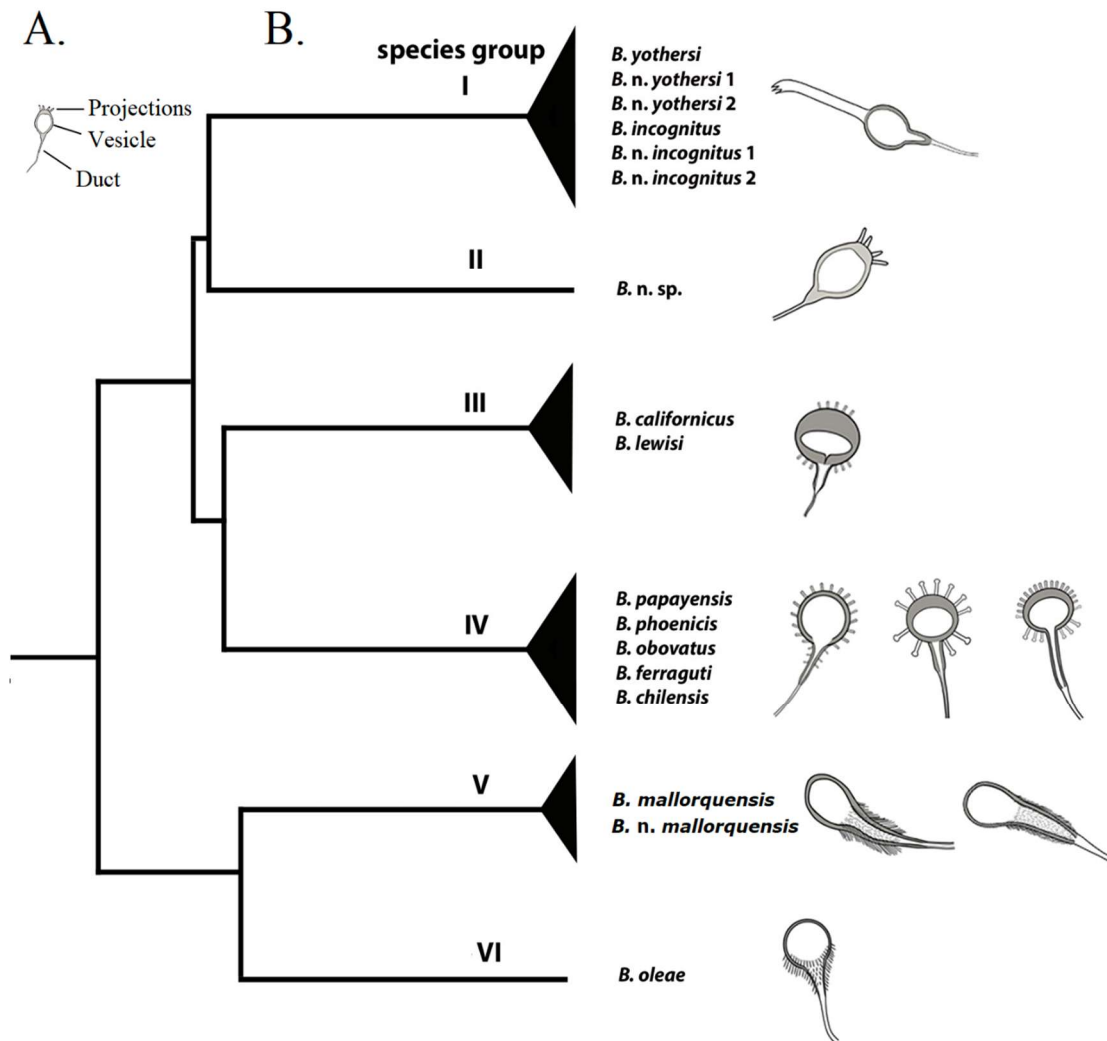
818 Among the morphological characters recently considered in the taxonomy of *Brevipalpus*
819 (Navia *et al.*, 2013; Beard *et al.*, 2015; Alves *et al.*, 2019) and described in **Table SM2-20, Figures**
820 **4A, 4B and SM1-10**, we conclude that cuticular patterns of the dorsal and ventral shields,
821 microplate ornamentation (**Figure SM1-11**), and the shape of the palp femurogenu seta are
822 species-specific. These characteristics vary among species within the same phylogenetic group,
823 and therefore are not phylogenetically informative at the species group level.

824 **Spermatheca character and its implications for the recognition of groups in *Brevipalpus***

825 Tree analyses supported the spermathecal patterns as a reliable and suited criterion for
826 distinguishing species groups (**Figures 4A and 4B, SM1-10 and 12; Table SM2-20**). The shape
827 of the seminal vesicle was homologous among closely related taxa within the same Clade (**Figure**
828 **4B; SM1-10 and 12**). The spermatheca or seminal receptacle is a part of the female insemination
829 system whose function is to store and protect the male sperm until its use in egg fertilization (Alberti
830 & Kitajima, 2014). The importance of the spermatheca in the taxonomy of *Brevipalpus* and other
831 tenuipalpids has been largely ignored for a long time. Castagnoli (1974) was the first to describe
832 in detail this organ in eight flat mite species, although she did not mention its taxonomic
833 importance. Later, Baker & Tuttle (1987) briefly described and illustrated the spermatheca in some
834 tenuipalpids from Mexico, including eight species in *Brevipalpus*, without using it for species
835 delimitation. Recent studies (Beard *et al.*, 2015; Di Palma *et al.*, 2020) have highlighted the
836 spermatheca as a key morphological character in species descriptions (Navia *et al.*, 2013; Beard
837 *et al.*, 2015; Alves *et al.*, 2019). In other plant mite groups, the spermatheca has long been
838 recognized as a valuable taxonomic trait, as females retain spermatozooids internally until the
839 conditions are favorable for egg production. The shape of the spermatheca is used to differentiate
840 species in predatory mites of the family Phytoseiidae and can also help to characterize species
841 groups or genera (Ragusa & Athias-Henriot, 1983; Chant & McMurtry, 2007). The internal position
842 of the spermatheca makes its morphology less susceptible to hereditary modifications than
843 external traits in direct contact with the environment (Athias-Henriot, 1977).

844 The findings of this study show that *Brevipalpus* species included in the species Group I have
845 an oval, thin-walled spermatheca with a smooth outer surface and a long (at least twice as long as
846 the vesicle), thick stipe on the distal pole (**Figure SM1-10A to 10F; SM1-12 and 13**); the single
847 species in Group II has a rounded, thin-walled spermatheca, with a crown of projections in the
848 distal pole (**Figure SM1-10G**); species in the Group III have a subspherical spermatheca,
849 somewhat flattened, thick-walled in the distal part leaving a reduced inner space, with short
850 projections in the proximal and distal poles (**Figure SM1-10H to 10K**); species in Group IV have a

851 flattened, thin-walled spermatheca in the distal part, covered by projections on the entire surface;
 852 distal projections are shorter and directed forward, proximal projections longer, finger-like, and
 853 directed backward (**Figure SM1-10L to 10P**); species in the Group V have a piriform spermatheca,
 854 with a broad base and covered with fine projections in the proximal half (**Figure SM1-10Q and**
 855 **10R**); and species in Group VI have a rounded spermatheca with a narrow base and fine
 856 projections on the proximal half (**Figure SM1-10S**). Although there is a high correlation between
 857 the shape of the female spermatheca and the genetic grouping; to avoid further confusion, the
 858 morphology of this structure should not be used in isolation for species-group identification, but in
 859 combination with other reliable traits.
 860



861
 862
 863 **Figure 4. A.** Spermathecal morphology, including a duct, a vesicle, and projections or ornamentation
 864 in the distal end. **B.** Tree representation showing the phylogenetic relationships among *Brevipalpus*
 865 species and candidate species based on concatenated datasets (*COI* barcoding, *COI* DNF-DNR,
 866 subunit D1–D3, and ITS2) and the morphology of the spermathecal vesicle is shown on the right for
 867 each Clade.
 868

869 **Cryptic diversity unveiled by multiple approaches: Incongruences suggest ongoing**
 870 **speciation**

871 Phylogenies and all species delimitation methods supported the presence of cryptic diversity
 872 in certain taxa. (**Figure 3**). *Brevipalpus n. mallorquensis* was confirmed to be a separate species
 873 by all species-delimitation methods used, supporting the findings of Alves *et al.* (2019). The DNA
 874 sequences of the specimens identified as *B. californicus* also suggest the existence of cryptic

875 species within the taxon. This information corroborates the findings of morphological studies by
876 Beard *et al.* (2012), who identified four morphotypes within the *B. californicus*, namely, *B.*
877 *californicus* s.l., *B. californicus* s.s., *B. californicus* species B, and *B. californicus* species C. The
878 congruences among multiple species-delimitation methods used in this study support the
879 hypothesis of new taxa, whose description is in preparation.

880 However, for some taxa, particularly in Clades I and IV, there were uncertainties between the
881 species-delimitation methods applied (**Figure 3**). Although the phylogenetic trees and
882 concatenated ones showed strong clustering at the *Brevipalpus* species level, some putative
883 species could not be differentiated through phylogenetic analyses (BPP \geq 98%) or by some of the
884 distance genetic techniques implemented. Generally, there was an overestimation of the number
885 of lineages when using delimitation approaches besides phylogeny and formal morphology (see
886 **Figure 3, Table SM2-20**).

887 The discordance between the mitochondrial and nuclear markers could be attributed to
888 incomplete lineage sorting, sex-biased dispersal, asymmetrical introgression, natural selection, or
889 genetic sweeps mediated by cytoplasmic bacteria (Després, 2019), such as *Cardinium* (Kitajima
890 *et al.*, 2007). Low mitochondrial diversity was observed in populations with high penetrance of
891 symbiotic bacteria like *Wolbachia* (Deng *et al.*, 2021), which could have affected the results of the
892 delimitation methods. The various transmission modes of mitochondrial and nuclear markers
893 (maternal *versus* biparental) could explain their differences in sensitivity in the population analysis
894 over time. Mitochondrial DNA is maternally inherited and does not undergo recombination, thus it
895 represents a single lineage, whereas nuclear DNA is inherited from both parents, undergoes
896 recombination, and could mix genetic material, potentially obscuring lineage boundaries (Després,
897 2019). The transplantation experiments conducted with *B. phoenicis* on various host plants
898 suggest that the clonal adaptation of these mites could be explained by the frozen niche variation
899 model (Groot *et al.*, 2005). This model proposes that clones specialized in various niches best
900 explain the clonal adaptation of these mites. Lineages within *B. yothersi* (detected only by *COI*
901 sequences), similar to those from *Cecropia*, and within *B. n. yothersi* 2, such as *Delonix* and *Citrus*,
902 could be explained by frozen niche variation.

903 These uncertainties or lack of effective congruence suggest that some speciation processes
904 are still in progress and that this study “captured” distinct phases of these processes, such as
905 those designated as *B. near yothersi* and *B. near incognitus* in Group I. Limited knowledge of the
906 ecological traits, distribution, host range, and reproduction mode of *Brevipalpus* mites hinders a
907 detailed discussion of the drivers and mechanisms of speciation events. Despite this, some
908 hypotheses could be proposed.

909 Results of species delimitation in populations morphologically identified as *B. incognitus*
910 suggest a nonadaptive radiation process, indicating lineage diversification without significant
911 ecological divergence (e.g., same host plant and geographic overlap). *Brevipalpus incognitus* was
912 originally described from coconut trees in southeastern Brazil (Navia *et al.*, 2013) and has not been
913 reported in other countries. Subsequently, it was also found on *Annona muricata* and *Phoenix* sp.
914 ornamental palms in the north and southeastern region of the country, respectively. Surprisingly,
915 specimens collected from the same host and locality as *B. incognitus* and identified as *B.*
916 *incognitus* consisted of different phylogenetic lineages, i.e., *B. near incognitus* 1 and 2. These
917 genetic lineages seems not exhibit ecological differences. This is the clearest example among the
918 studied putative species of the occurrence of nonadaptive radiation, but it could be a common
919 process for *Brevipalpus* mites. Although adaptative radiation has long been considered the
920 standard evolutionary pattern (Losos & Mahler, 2010), nonadaptive radiations are also common
921 and are genuine phenomena related to the properties of organisms as well as to ecological
922 conditions (Czekanski-Moir & Rundell, 2019). Nonadaptive radiation generally involves the
923 proliferation of species that can occur as a result of the restriction of gene flow (Czekanski-Moir &
924 Rundell, 2019). Limited information is available on the reproductive behavior of *Brevipalpus* mites,
925 as only a few economically important species have been studied. In species such as *B. chilensis*
926 (Group IV), the female to male ratio is nearly 1:1, with sexual reproduction (Alberti *et al.*, 2014)
927 and no observed presence of *Cardinium* (Quiros-Gonzalez, 1986). Males are more prevalent in
928 species from the *cuneatus* (Group V) and *sportalis* groups, which encompass most of the genus’s
929 diversity, whereas males are rare in other groups.

930 One reason for reproductive isolation is the cytoplasmic incompatibility (CI) caused by
931 symbionts. Infections by *Cardinium* and *Wolbachia* have cause CI in numerous arthropods

932 (Shropshire et al., 2020), including mites (Gotoh et al., 2007; Cruz et al., 2021). In addition to
933 *Cardinium*, *Wolbachia* has been found in the *Brevipalpus* bacteriome (Ospina et al., 2016).
934 Although *Cardinium* does not cause CI in *B. yothersi*, it is possible that variants infesting other
935 species could cause it. Therefore, it is most likely that CI induced by symbionts drives speciation
936 for some *Brevipalpus* mites, as has been demonstrated for other arthropods (Bordenstein et al.,
937 2001; Jaenike et al., 2006). Additionally, other mechanisms of reproductive isolation between
938 haplodiploid spider mite populations (belonging to the family Tetranychidae) are under
939 investigation (Cruz et al., 2021; Engelstädter & Hurst, 2009; Knegt et al., 2016; Cruz et al., 2021)
940 and may be clues to analyze similar processes in *Brevipalpus*. Studies comparing the importance
941 of the mode of reproduction linked to the phylogenies are rare. A comparison of sexual
942 monogononta rotifers and obligately asexual bdelloid (Tang et al., 2014) is consistent with the
943 hypothesis that bdelloid diversified at a faster rate into less discrete species because their
944 diversification does not depend on the evolution of reproductive isolation. This highlights other
945 points to explore for *Brevipalpus* populations.

946 The results also suggested cryptic speciation in populations closely related to the
947 parthenogenetic species *B. yothersi* (Alberti et al., 2014) associated with citrus in Argentina and
948 Brazil. In this case, adaptative radiation may have occurred when populations became physically
949 isolated from each other for a long time or due to underlying divergent selection for adaptation to
950 different niches (adaptative radiation), as reported for oribatid parthenogenetic mites (Birky &
951 Barraclough, 2009; Heethoff et al., 2009). Although the new genetic lineages can be phenotypically
952 distinct in these soil-dwelling mites, some cases of cryptic speciation detected only by genetic
953 analysis have also been reported (Birky & Barraclough, 2009). Maraun et al. (2003) observed that
954 the differences between closely related parthenogenetic species were larger than those between
955 closely related sexual species, indicating that parthenogenetic lineages may radiate slower than
956 sexual species.

957 **DNA barcoding for *Brevipalpus***

958 In this study, the distance values corroborated some putative species and were variable
959 according to the gene fragment or region used. Some *Brevipalpus* species have shown maximum
960 intraspecific divergences equal to or greater than the minimum and mean interspecific distances,
961 indicating an overlap between the maximum intra- and minimum interspecific values. The highest
962 intraspecific divergence (K-2P) in *COI* barcoding was observed within *B. yothersi* sequences
963 (2.44%), surpassing the mean and minimum divergence between *B. n. yothersi* 1 and *B. n. yothersi*
964 2 (\underline{X} distance = 2.22%, 1.99%–2.44%) and between *B. n. incognitus* 1 and *B. n. incognitus* 2 (\underline{X}
965 distance = 1.99%, 1.99%–1.99%). There was no overlap of these values in the other species and
966 putative species. In the *COI* DNF-DNR fragment, the highest intraspecific variability occurred
967 within *B. yothersi* (4.28%) and *B. papayensis* (3.48%). These values exceeded most of the
968 minimum interspecific distances and some of the mean distances obtained for species grouped in
969 Clade IV. Some closely related species (e.g., *B. yothersi* versus *B. incognitus*, *B. chilensis* x *B.*
970 *obovatus*) showed extensive amounts of intraspecific variation, often exceeding the interspecific
971 variation between the species (Table 3; SM2-11–SM2-18). Therefore, the general barcoding
972 assumption that intraspecific variation is smaller than interspecific variation was disregarded for
973 some *Brevipalpus* species, as previously reported in the genus *Tetranychus* (Ros & Breeuwer,
974 2007).

975 **The boundaries of the species delimitation**

976 Establishing GD thresholds within and between species is important for molecular diagnostics
977 of *Brevipalpus* species (Table 6). Based on the *COI* barcoding sequences, the lowest GDs
978 between *B. chilensis* vs *B. ferraguti* and *B. chilensis* vs *B. obovatus* were 2.68% and 2.90%,
979 respectively, which were above $y = 2.54\%$. These species are morphologically distinct, and there
980 is no doubt about their identification, thus, $\alpha = 3.27\%$ could be a reliable value to differentiate
981 species. The selection of the CI-max value (3.95%) enhances the security of confirming genetic
982 distinctiveness of species. The *COI* DNF-DNR showed $y = 3.34$ (1.31%–5.73%). Above this
983 intersection point (y), only valid species were observed. However, the intraspecific variability within
984 *B. yothersi* and *B. papayensis* was high, at 4.28% and 3.48%, respectively. In studies based solely
985 on DNA sequences, values between α (3.27%) and CI-max (5.73%) could also indicate genetic

986 differentiation of *Brevipalpus* species. The variability values for subunit D1–D3 were lower than
987 those for the mitochondrial regions, with $y = 1.76\%$ (0.7%–2.82%). The shortest genetic distances
988 separating two valid species were 0.40% (*B. yothersi* vs *B. incognitus*) and 1.2% (*B. papayensis*
989 vs *B. phoenicis*). Likewise, the $\alpha = 2.07\%$ and CI-max = 2.82% for the subunit D1–D3 indicates a
990 reliable differentiation between species. The values for the ITS2 region were higher, with $y = 7.75\%$
991 (4.37–11.14%). Although closely related species showed a low ITS2 threshold value, i.e., *B.*
992 *californicus* s.s. versus *B. lewisi* (0.93%), high intraspecific distances were recorded in *B.*
993 *papayensis* (4.83%, 0–13.07%), *B. obovatus* (6.90%, 0–12.51%), and *B. chilensis* (3.73%, 0%–
994 11.43%), causing the estimated value for y to shift upward. This supports the presence of distinct
995 lineages within these taxa as detected by ABDG and ASAP. Based on these findings, a threshold
996 value up to $y = 7.75\%$ and 11.14% (CI-max) could be used for ITS2 molecular diagnostic studies
997 in the absence of morphological data (Table 6). The description of the new valid species will lower
998 these threshold values.

999 Findings of previous studies on plant mites provided reference values for comparison with the
1000 findings of this study. Two closely related species of phytophagous spider mites, *Tetranychus*
1001 *urticae* and *T. turkestanii* (Ugarov & Nikolski), exhibited significant nucleotide diversity in the *COI*
1002 region (mtDNA) (3%–4%) and minimal variation in the ITS2 region (<0.5%) (Navajas et al., 1998).
1003 Intraspecific values for single species were as follows: *Tetranychus evansi* (Baker & Pritchard)
1004 populations showed *COI* diversity ranging from 0.03% to 1.4% (Boubou et al., 2011);
1005 *Eotetranychus carpini* (Oudemans) populations presented ITS nucleotide diversity of 0.6%
1006 (Malagnini et al., 2012); *Aceria guerreronis* (Keifer) from different geographic regions worldwide
1007 exhibited ITS nucleotide diversity ranging from 0.49% to 1.90% (Navia et al., 2005); the predatory
1008 mite *Euseius nicholsi* (Ehara & Lee) had *COI* nucleotide diversity ranging from 0.342% to 1.11%
1009 and ITS nucleotide diversity ranging from 0.0% to 0.19% (Yang et al., 2012). High interspecific
1010 variation in the ITS region has been reported in the following Phytoseiidae species: *Typhlodromus*
1011 *phialatus* Athias-Henriot/*T. pyri* Scheuten (6.7%) (Tixier et al., 2006); *Amblyseius largoensis*
1012 (Muma)/*A. herbicolus* (Chant) (5.89%) (Navia et al., 2014), and *Neoseiulella aceris* (Collyer)/*N.*
1013 *litoralis* (Swirski & Amitai) (6.0%) (Kanouh et al., 2010). The results for *Brevipalpus* were in line
1014 with previously reported values for mitochondrial markers, and this study revealed new values for
1015 the subunit D1–D3. The ITS2 sequences showed high variability among the species examined.
1016 The proposed threshold values for *Brevipalpus* species streamline species assignment by linking
1017 sequence clusters with taxa, thereby facilitating taxonomic studies in cases of uncertain
1018 classifications.

1019

Final considerations

1020 This study provided, for the first time, a phylogenetic background that allowed revisiting the
1021 species group concept in the genus *Brevipalpus*, previously based on a few morphological
1022 characters and therefore artificial. Multi-locus genetic distances were analyzed through a variety
1023 of approaches to identify cryptic lineages, support species diagnosis, and highlight priority study
1024 needs. The revealed speciation in two *Brevipalpus* species groups (I and IV) not linked to
1025 ecological differences makes this group of mites an excellent model for evolutionary studies
1026 focusing on reproductive modes and endosymbionts.

1027 The importance of an integrative approach to advancing the systematics of *Brevipalpus* mites
1028 is emphasized by the results of this study. It was noted that nuclear markers were essential for
1029 identifying species lineages and detecting host-associated lineages when mitochondrial DNA did
1030 not exhibit enough diversity. However, nuclear markers were unable to detect cryptic diversity
1031 within *B. yothersi* and *B. incognitus*, strongly suggested by the mitochondrial fragments.
1032 Additionally, both nuclear and mitochondrial markers were crucial and complemented each other
1033 in identifying candidate lineages linked to hosts in *B. chilensis* and *B. obovatus* when morphological
1034 evidence was lacking. Therefore, it is important to carefully consider the markers and model to use
1035 in species delimitation before asserting the occurrence of new cryptic species (Després, 2019) and
1036 morphological investigations remain crucial for evaluating genetic differences in potential new
1037 species.

1038 The inclusion of new species, populations, and the enrichment of sequence datasets will
1039 certainly validate the threshold values given in this study. In any case, the ranges established are
1040 already quite reliable and can be used to support routine taxonomic identifications, such as

1041 pinpointing cryptic lineages, identifying specimens intercepted in transit of plant material, or for
1042 field surveys to detect vector species. It is advisable to consider all of these findings within an
1043 integrative taxonomy framework.

1044 **Legal requirements**

1045 DN obtained a permanent license, Permit Number 20650-1, from ICMBio (Chico Mendes
1046 Institute for the Conservation of Biodiversity, Brazilian Ministry for Environment) for collecting
1047 zoological specimens in Brazil.

1048 **Appendices**

1049 [Revisiting the systematics of *Brevipalpus* mites Supplementary Material 1, Figures -SM1](#)
1050 [\(hal-04907419\)](#)

1051
1052 [Revisiting the systematics of *Brevipalpus* mites Supplementary Material 2, Tables -SM2](#)
1053 [\(hal-04907419\)](#)

1054
1055 Mitochondrial (COI barcoding & COI DNF/DNR) and nuclear (D1-D3 28S & ITS2) DNA datasets:
1056 Revisiting the systematics of *Brevipalpus* mites <https://doi.org/10.5281/zenodo.14722287>
1057

1058 **Acknowledgements**

1059 We offer special thanks Prof. Dr. Manoel Guedes Correa Gondim Jr., Dra. Rosa de Belém das
1060 Neves Alves, and Roberto C. Trincado for their help with sample collection. We also appreciate
1061 the contributions of Prof. Dr. Elliot Watanabe from Escola Superior de Agricultura “Luiz de
1062 Queiroz”, ESALQ-USP, Piracicaba, São Paulo, for his assistance in collecting specimens for the
1063 study and for supporting the scanning electron microscopy studies. We thank Dr. Gregory Evans
1064 (APHIS-USDA) for his valuable input and expertise in revising the manuscript. We thank
1065 EMBRAPA, the University of São Paulo, the Smithsonian National Museum of Natural History, and
1066 the National Agricultural Library (NAL-USDA) for their support and assistance with references.
1067 Mention of trade names or commercial products in this publication is solely for the purpose of
1068 providing specific information and does not imply recommendation or endorsement by the USDA;
1069 USDA is an equal opportunity provider and employer.

1070 **Funding**

1071 The Brazilian Coordination for the Improvement of Higher Education Personnel (CAPES),
1072 National Program of PostDoctoral in Agronomy, Brazil for providing financial support for RSM
1073 (CAPES-PNPD/Agronomy Proc. No. 88882.305808/2018-1) and National Council for Scientific
1074 and Technological Development (CNPQ) (Proc No. 161389/2011-2). The project ‘Genomics and
1075 transcriptomic of virus-vector-host plant relationship in the pathosystem of *Brevipalpus* transmitted
1076 viruses; systematic and evolution of *Brevipalpus* mites and their endosymbionts; new strategies to
1077 manage citrus leprosis in the São Paulo state’ (FAPESP, the São Paulo Research Foundation,
1078 Proc No. 2019/25078-9).

1079 **Conflict of interest disclosure**

1080 The authors declare that they comply with the PCI rule of having no financial conflicts of interest
1081 in relation to the content of the article.

1082 **References**

1083 Alberti G, Kitajima EW (2014) Anatomy and fine structure of *Brevipalpus* mites (Tenuipalpidae) -

1084 economically important plant-virus vectors. *Zoologica*, **160**, 192.

1085 Alberti G, Tassi AD, Kitajima EW (2014) Anatomy and fine structure of *Brevipalpus* mites

1086 (Tenuiplapidae) – economically important plant-virus vectors – part 6: female reproductive system.

1087 *Zoologica.*, **160**, 145–172.

1088 Alves JL dos S, Ferragut F, Mendonça RS, Tassi AD, Navia D (2019) A new species of *Brevipalpus*

1089 (Acari: Tenuipalpidae) from the Azores Islands, with remarks on the *B. cuneatus* species group.

1090 *Systematic and Applied Acarology*, **24**, 2184–2208. <https://doi.org/10.11158/saa.24.11.10>

1091 Athias-Henriot C (1977) Nouvelles notes sur les Amblyseïini III. Sur le genre *Cydnodromus*:

1092 redéfinition, composition [Parasitiformes, Phytoseiidae]. *Entomophaga*, **22**, 61–73.

1093 <https://doi.org/10.1007/BF02372991>

1094 Austerlitz F, David O, Schaeffer B, Bleakley K, Olteanu M, Leblois R, Veuille M, Laredo C (2009)

1095 DNA barcode analysis: a comparison of phylogenetic and statistical classification methods. *BMC*

1096 *Bioinformatics*, **10**, S10. <https://doi.org/10.1186/1471-2105-10-S14-S10>

1097 Baker EW, Tuttle DM (1987) *The False Spider Mites of Mexico (Tenuipalpidae: Acari)*.

1098 Baker EW, Tuttle DM, Abbatiello M (1975) The false spider mites of northwestern and north central

1099 Mexico (Acarina, Tenuipalpidae). *Smithsonian Contributions to Zoology*, 1–23.

1100 <https://doi.org/10.5479/si.00810282.194>

1101 Beard JJ, Ochoa R, Bauchan GR, Trice MD, Redford AJ, Walters TW, Mitter C (2012) Flat Mites

1102 of the world. *Identification Technology Program, CPHST, PPQ, APHIS, USDA; Fort Collins, CO*.

1103 Beard JJ, Ochoa R, Braswell WE, Bauchan GR (2015) *Brevipalpus phoenicis* (Geijskes) species

1104 complex (Acari: Tenuipalpidae)—a closer look. *Zootaxa*, **3944**, 1.

1105 <https://doi.org/10.11646/zootaxa.3944.1.1>

1106 Birky CWJ, Barraclough TG (2009) Asexual Speciation. In: *Lost Sex The Evolutionary Biology of*

1107 *Parthenogenesis*, pp. 201–216. Springer Netherlands, Dordrecht. [https://doi.org/10.1007/978-90-481-](https://doi.org/10.1007/978-90-481-2770-2_10)

1108 [2770-2_10](https://doi.org/10.1007/978-90-481-2770-2_10)

1109 Bordenstein SR, O'Hara FP, Werren JH (2001) *Wolbachia*-induced incompatibility precedes other

1110 hybrid incompatibilities in *Nasonia*. *Nature*, **409**, 707–710.

1111 Boubou A, Migeon A, Roderick GK, Navajas M (2011) Recent emergence and worldwide spread

1112 of the red tomato spider mite, *Tetranychus evansi*: genetic variation and multiple cryptic invasions.

1113 *Biological Invasions*, **13**, 81–92. <https://doi.org/10.1007/s10530-010-9791-y>

1114 Castagnoli M (1974) La spermateca in alcune specie di Brevipalpini (Acarina, Tenuipalpidae).

1115 *Redia*, **55**, 85–88.

1116 Castro EB, Mesa NC, Feres RJF, Moraes GJ d., Ochoa R, Beard JJ, Demite PR (2024)

1117 Tenuipalpidae Database. <https://doi.org/10.11646/zootaxa.4868.4.7>

1118 Chant DA, McMurtry JA (2007) *Illustrated Keys and Diagnoses for the Genera and Subgenera of*

1119 *the Phytoseiidae of the World (Acari: Mesostigmata)*. Indira Publishing House, West Bloomfield,

1120 Michigan.

1121 Childers CC, Rodrigues JC. (2011) An overview of *Brevipalpus* mites (Acari: Tenuipalpidae) and

1122 the plant viruses they transmit. *Zoosymposia*, **6**, 180–192. <https://doi.org/10.11646/zoosymposia.6.1.28>

1123 Collins RA, Boykin LM, Cruickshank RH, Armstrong KF (2012) Barcoding's next top model: An

1124 evaluation of nucleotide substitution models for specimen identification. *Methods in Ecology and*

1125 *Evolution*, **3**, 457–465. <https://doi.org/10.1111/j.2041-210X.2011.00176.x>

1126 Cruz MA, Magalhães S, Sucena É, Zélé F (2021) *Wolbachia* and host intrinsic reproductive barriers

1127 contribute additively to postmating isolation in spider mites. *Evolution*, **75**, 2085–2101.

1128 <https://doi.org/10.1111/evo.14286>

1129 Czekanski-Moir JE, Rundell RJ (2019) The ecology of nonecological speciation and nonadaptive

1130 radiations. *Trends in Ecology & Evolution*, **34**, 400–415. <https://doi.org/10.1016/j.tree.2019.01.012>

1131 Darriba D, Taboada GL, Doallo R, Posada D (2012) jModelTest 2: more models, new heuristics

1132 and parallel computing. *Nature Methods*, **9**, 772–772. <https://doi.org/10.1038/nmeth.2109>

1133 Deng J, Assandri G, Chauhan P, Futahashi R, Galimberti A, Hansson B, Lancaster LT, Takahashi

1134 Y, Svensson EI, Duploux A (2021) *Wolbachia*-driven selective sweep in a range expanding insect

1135 species. *BMC Ecology and Evolution*, **21**, 181. <https://doi.org/10.1186/s12862-021-01906-6>

1136 Després L (2019) One, two or more species? Mitonuclear discordance and species delimitation.

1137 *Molecular Ecology*, **28**, 3845–3847. <https://doi.org/10.1111/mec.15211>

1138 Dowling APG, Ochoa R, Beard JJ, Welbourn WC, Ueckermann EA (2012) Phylogenetic

1139 investigation of the genus *Raoiella* (Prostigmata: Tenuipalpidae): Diversity, distribution, and world

1140 invasions. *Experimental and Applied Acarology*, **57**, 257–269. [https://doi.org/10.1007/s10493-011-](https://doi.org/10.1007/s10493-011-9483-z)

1141 [9483-z](https://doi.org/10.1007/s10493-011-9483-z)

1142 Edgar RC (2004) MUSCLE: multiple sequence alignment with high accuracy and high throughput.

1143 *Nucleic Acids Research*, **32**, 1792–1797. <https://doi.org/10.1093/nar/gkh340>

1144 Engelstädter J, Hurst GDD (2009) The ecology and evolution of microbes that manipulate host
1145 reproduction. *Annual Review of Ecology, Evolution, and Systematics*, **40**, 127–149.
1146 <https://doi.org/10.1146/annurev.ecolsys.110308.120206>

1147 Folmer O, Black M, Hoeh W, Lutz R, Vrijenhoek R (1994) DNA primers for amplification of
1148 mitochondrial cytochrome c oxidase subunit I from diverse metazoan invertebrates. *Molecular Marine*
1149 *Biology and Biotechnology*, **3**, 294–299.

1150 Gasteiger E (2003) ExpASy: the proteomics server for in-depth protein knowledge and analysis.
1151 *Nucleic Acids Research*, **31**, 3784–3788. <https://doi.org/10.1093/nar/gkg563>

1152 Gilbert GS, Webb CO (2007) Phylogenetic signal in plant pathogen–host range. *Proceedings of*
1153 *the National Academy of Sciences*, **104**, 4979–4983. <https://doi.org/10.1073/pnas.0607968104>

1154 Godefroid M, Rocha S, Santos H, Paiva M-R, Burbano C, Kerdelhué C, Branco M, Rasplus J-Y,
1155 Rossi J-P (2016) Climate constrains range expansion of an allochronic population of the pine
1156 processionary moth (A Andersen, Ed.). *Diversity and Distributions*, **22**, 1288–1300.
1157 <https://doi.org/10.1111/ddi.12494>

1158 Gotoh T, Noda H, Ito S (2007) *Cardinium* symbionts cause cytoplasmic incompatibility in spider
1159 mites. *Heredity*, **98**, 13–20. <https://doi.org/10.1038/sj.hdy.6800881>

1160 Grandjean F (1939) Les segments post-larvaires de l'hystérosoma chez les Oribates (Acariens).
1161 *Les segments post-larvaires de l'hystérosoma chez les Oribates (Acariens)*, **64**, 273–284.

1162 Grbić M, Van Leeuwen T, Clark RM, Rombauts S, Rouzé P, Grbić V, Osborne EJ, Dermauw W,
1163 Ngoc PCT, Ortego F, Hernández-Crespo P, Diaz I, Martínez M, Navajas M, Sucena É, Magalhães S,
1164 Nagy L, Pace RM, Djuranović S, Smagghe G, Iga M, Christiaens O, Veenstra JA, Ewer J, Villalobos
1165 RM, Hutter JL, Hudson SD, Velez M, Yi S V., Zeng J, Pires-Da Silva A, Roch F, Cazaux M, Navarro M,
1166 Zhurov V, Acevedo G, Bjelica A, Fawcett JA, Bonnet E, Martens C, Baele G, Wissler L, Sanchez-
1167 Rodriguez A, Tirry L, Blais C, Demeestere K, Henz SR, Gregory TR, Mathieu J, Verdon L, Farinelli L,
1168 Schmutz J, Lindquist E, Feyereisen R, Van De Peer Y (2011) The genome of *Tetranychus urticae*
1169 reveals herbivorous pest adaptations. *Nature*, **479**, 487–492. <https://doi.org/10.1038/nature10640>

1170 Groot TVM, Breeuwer JAJ (2006) *Cardinium* symbionts induce haploid thelytoky in most clones of
1171 three closely related *Brevipalpus* species. *Experimental and Applied Acarology*, **39**, 257–271.
1172 <https://doi.org/10.1007/s10493-006-9019-0>

1173 Groot TVM, Janssen A, Pallini A, Breeuwer JAJ (2005) Adaptation in the Asexual False Spider
1174 Mite *Brevipalpus phoenicis*: Evidence for Frozen Niche Variation. *Experimental and Applied Acarology*,
1175 **36**, 165–176. <https://doi.org/10.1007/s10493-005-3360-6>

1176 Guindon S, Dufayard JF, Lefort V, Anisimova M, Hordijk W, Gascuel O (2010) New algorithms and
1177 methods to estimate maximum-likelihood phylogenies: Assessing the performance of PhyML 3.0.
1178 *Systematic Biology*, **59**, 307–321. <https://doi.org/10.1093/sysbio/syq010>

1179 Guindon S, Gascuel O (2003) A Simple, Fast, and Accurate Algorithm to Estimate Large
1180 Phylogenies by Maximum Likelihood (B Rannala, Ed.). *Systematic Biology*, **52**, 696–704.
1181 <https://doi.org/10.1080/10635150390235520>

1182 Hall TA (1999) BioEdit: A User-Friendly Biological Sequence Alignment Editor and Analysis
1183 Program for Windows 95/98/NT. *Nucleic Acids Symposium Series*, **41**.

1184 Hebert PDN, Cywinska A, Ball SL, DeWaard JR (2003) Biological identifications through DNA
1185 barcodes. *Proceedings of the Royal Society of London. Series B: Biological Sciences*, **270**, 313–321.
1186 <https://doi.org/10.1098/rspb.2002.2218>

1187 Hebert PDN, Penton EH, Burns JM, Janzen DH, Hallwachs W (2004) Ten species in one: DNA
1188 barcoding reveals cryptic species in the neotropical skipper butterfly *Astraptes fulgerator*. *Proceedings*
1189 *of the National Academy of Sciences*, **101**, 14812–14817. <https://doi.org/10.1073/pnas.0406166101>

1190 Heethoff M, Norton RA, Scheu S, Maraun M (2009) *Parthenogenesis in Oribatid mites (Acari,*
1191 *Oribatida): evolution without sex* (I Schön, K Martens, P Dijk, Eds.). Springer Netherlands, Dordrecht.
1192 <https://doi.org/10.1007/978-90-481-2770-2>

1193 Huemer P, Mutanen M, Sefc KM, Hebert PDN (2014) Testing DNA Barcode Performance in 1000
1194 Species of European Lepidoptera: Large Geographic Distances Have Small Genetic Impacts (B
1195 Schierwater, Ed.). *PLoS ONE*, **9**, e115774. <https://doi.org/10.1371/journal.pone.0115774>

1196 Jaenike J, Dyer KA, Cornish C, Minhas MS (2006) Asymmetrical reinforcement and *Wolbachia*
1197 infection in *Drosophila* (M Noor, Ed.). *PLoS Biology*, **4**, e325.
1198 <https://doi.org/10.1371/journal.pbio.0040325>

1199 Jin P-Y, Sun J-T, Hoffmann A, Guo Y-F, Zhou J-C, Zhu Y-X, Chen L, Hong X-Y (2019)
1200 Phylogenetic signals in pest abundance and distribution range of spider mites. *BMC Evolutionary*
1201 *Biology*, **19**, 223. <https://doi.org/10.1186/s12862-019-1548-3>

1202 Jörger KM, Norenburg JL, Wilson NG, Schrödl M (2012) Barcoding against a paradox? Combined
1203 molecular species delineations reveal multiple cryptic lineages in elusive meiofaunal sea slugs. *BMC*

1204 *Evolutionary Biology*, **12**, 245. <https://doi.org/10.1186/1471-2148-12-245>

1205 Jorna J, Linde JB, Searle PC, Jackson AC, Nielsen M-E, Nate MS, Saxton NA, Grewe F, Herrera-

1206 Campos M de los A, Spjut RW, Wu H, Ho B, Lumbsch HT, Leavitt SD (2021) Species boundaries in

1207 the messy middle—A genome-scale validation of species delimitation in a recently diverged lineage of

1208 coastal fog desert lichen fungi. *Ecology and Evolution*, **11**, 18615–18632.

1209 <https://doi.org/10.1002/ece3.8467>

1210 Kanouh M, Tixier M-S, Guichou S, Brigitte C, Kreiter S (2010) Two synonymy cases within the

1211 genus *Neoseiulella* (Acari: Phytoseiidae): is the molecular evidence so evident? *Biological Journal of*

1212 *the Linnean Society*, **101**, 323–344. <https://doi.org/10.1111/j.1095-8312.2010.01516.x>

1213 Kekkonen M, Mutanen M, Kaila L, Nieminen M, Hebert PDN (2015) Delineating Species with DNA

1214 barcodes: a case of taxon dependent method performance in moths (B Schierwater, Ed.). *PLOS ONE*,

1215 **10**, e0122481. <https://doi.org/10.1371/journal.pone.0122481>

1216 Kellermann V, Overgaard J, Hoffmann AA, Fløjgaard C, Svenning J-C, Loeschcke V (2012) Upper

1217 thermal limits of *Drosophila* are linked to species distributions and strongly constrained phylogenetically.

1218 *Proceedings of the National Academy of Sciences*, **109**, 16228–16233.

1219 <https://doi.org/10.1073/pnas.1207553109>

1220 Kimura M (1980) A simple method for estimating evolutionary rates of base substitutions through

1221 comparative studies of nucleotide sequences. *Journal of Molecular Evolution*, **16**, 111–120.

1222 <https://doi.org/10.1007/BF01731581>

1223 Kitajima EW, Groot TVM, Novelli VM, Freitas-Astúa J, Alberti G, de Moraes GJ (2007) In situ

1224 observation of the *Cardinium* symbionts of *Brevipalpus* (Acari: Tenuipalpidae) by electron microscopy.

1225 *Experimental and Applied Acarology*, **42**, 263–271. <https://doi.org/10.1007/s10493-007-9090-1>

1226 Kitajima EW, Rodrigues JCV, Freitas-Astua J (2010) An annotated list of ornamentals naturally

1227 found infected by *Brevipalpus* mite-transmitted viruses. *Scientia Agricola*, **67**, 348–371.

1228 <https://doi.org/10.1590/S0103-90162010000300014>

1229 Knegt B, Potter T, Pearson NA, Sato Y, Staudacher H, Schimmel BCJ, Kiers ET, Egas M (2016)

1230 Detection of genetic incompatibilities in non-model systems using simple genetic markers: hybrid

1231 breakdown in the haplodiploid spider mite *Tetranychus evansi*. *Heredity*, **118**, 311–321.

1232 [doi:10.1038/hdy.2016.103](https://doi.org/10.1038/hdy.2016.103)

1233 Kumar S, Stecher G, Tamura K (2016) MEGA7: Molecular Evolutionary Genetics Analysis version

1234 7.0 for bigger datasets. *Molecular Biology and Evolution*, **33**, 1870–1874.

1235 <https://doi.org/10.1093/molbev/msw054>

1236 Van Leeuwen T, Vanholme B, Van Pottelberge S, Van Nieuwenhuysse P, Nauen R, Tirry L,

1237 Denholm I (2008) Mitochondrial heteroplasmy and the evolution of insecticide resistance: Non-

1238 Mendelian inheritance in action. *Proceedings of the National Academy of Sciences*, **105**, 5980–5985.

1239 <https://doi.org/10.1073/pnas.0802224105>

1240 de Lillo E, Freitas-Astúa, Juliana; Watanabe Kitajima, Elliot; Ramos-González, Pedro Luis; Simoni

1241 S, Tassi, Aline Daniele; Valenzano D (2021) Phytophagous mites transmitting plant viruses: update and

1242 perspectives. *Entomologia Generalis*, **41**, 439–462. [10.1127/entomologia/2021/1283](https://doi.org/10.1127/entomologia/2021/1283)

1243 Lima DB, Rezende-Puker D, Mendonça RS, Tixier MS, Gondim MGC, Melo JWS, Oliveira DC,

1244 Navia D (2018) Molecular and morphological characterization of the predatory mite *Amblyseius*

1245 *largoensis* (Acari: Phytoseiidae): surprising similarity between an Asian and American populations.

1246 *Experimental and Applied Acarology*. <https://doi.org/10.1007/s10493-018-0308-1>

1247 Lindquist EE (1985) External anatomy. In: *Spider mites: Their Biology, Natural Enemies and*

1248 *Control* (eds Helle W, Sabelis M), pp. 3–28. Series: World Crop Pests, IA, Elsevier Science Publishers,

1249 Netherlands.

1250 Losos JB, Mahler DL (2010) Adaptive radiation: the interaction of ecological opportunity,

1251 adaptation, and speciation. In: *Evolution since Darwin: The First 150 Years* (eds Bell MA, Futuyma DJ,

1252 Eanes WF, Levinton JS), pp. 381–420. MA: Sinauer, Sunderland.

1253 Maddison WP, Maddison DR (2021) Mesquite: a modular system for evolutionary analysis. Version

1254 3.81 <http://www.mesquiteproject.org>

1255 Malagnini V, Navajas M, Migeon A, Duso C (2012) Differences between sympatric populations of

1256 *Eotetranychus carpini* collected from *Vitis vinifera* and *Carpinus betulus*: insights from host-switch

1257 experiments and molecular data. *Experimental and Applied Acarology*, **56**, 209–219.

1258 <https://doi.org/10.1007/s10493-012-9511-7>

1259 Maraun M, Heethoff M, Scheu S, Norton RA, Weigmann G, Thomas RH (2003) Radiation in sexual

1260 and parthenogenetic oribatid mites (Oribatida, Acari) as indicated by genetic divergence of closely

1261 related species. *Experimental and Applied Acarology*, **29**, 265–277.

1262 <https://doi.org/10.1023/A:1025833814356>

1263 Mendonça RS de, Navia D, Diniz IR, Auger P, Navajas M (2011) A critical review on some closely

1264 related species of *Tetranychus sensu stricto* (Acari: Tetranychidae) in the public DNA sequences
1265 databases. *Experimental and Applied Acarology*, **55**, 1–23. <https://doi.org/10.1007/s10493-011-9453-5>
1266 Mesa NC, Ochoa R, Welbourn WC, Evans GA, Moraes GJ de (2009) A catalog of the
1267 Tenuipalpidae (Acari) of the World with a key to genera. *Zootaxa*, **2098**, 1–185.
1268 <https://doi.org/10.11646/zootaxa.2098.1.1>
1269 Meyer MKPS (1979) The Tenuipalpidae (Acari) of Africa. With keys to the world fauna. *Entomology*
1270 *Memoir, Department of Agricultural Technical Services, Republic of South Africa*, **50**, 135.
1271 Meyer CP, Paulay G (2005) DNA barcoding: error rates based on comprehensive sampling (C
1272 Godfray, Ed.). *PLoS Biology*, **3**, e422. <https://doi.org/10.1371/journal.pbio.0030422>
1273 Navajas M, Gutierrez J, Lagnel J, Boursot P (1996) Mitochondrial cytochrome oxidase I in
1274 tetranychid mites: a comparison between molecular phylogeny and changes of morphological and life
1275 history traits. *Bulletin of Entomological Research*, **86**, 407–417.
1276 <https://doi.org/10.1017/S0007485300034994>
1277 Navajas M, Lagnel J, Fauvel G, Moraes GJ de (1999) Sequence variation of ribosomal internal
1278 transcribed spacers (ITS) in commercially important Phytoseiidae mites. *Experimental and Applied*
1279 *Acarology*, **23**, 851–859.
1280 Navajas M, Lagnel J, Gutierrez J, Boursot P (1998) Species-wide homogeneity of nuclear
1281 ribosomal ITS2 sequences in the spider mite *Tetranychus urticae* contrasts with extensive mitochondrial
1282 COI polymorphism. *Heredity*, **80**, 742–752. <https://doi.org/10.1046/j.1365-2540.1998.00349.x>
1283 Navia D, Domingos CA, Mendonça RS, Ferragut F, Rodrigues MAN, de Moraes EGF, Tixier M-S,
1284 Gondim MGC (2014) Reproductive compatibility and genetic and morphometric variability among
1285 populations of the predatory mite, *Amblyseius largoensis* (Acari: Phytoseiidae), from Indian Ocean
1286 Islands and the Americas. *Biological Control*, **72**, 17–29.
1287 <https://doi.org/10.1016/j.biocontrol.2014.01.011>
1288 Navia D, Mendonça RS, Ferragut F, Miranda LC, Trincado RC, Michaux J, Navajas M (2013)
1289 Cryptic diversity in *Brevipalpus* mites (Tenuipalpidae). *Zoologica Scripta*, **42**, 406–426.
1290 <https://doi.org/10.1111/zsc.12013>
1291 Navia D, de Moraes GJ, Roderick G, Navajas M (2005) The invasive coconut mite *Aceria*
1292 *guerreronis* (Acari: Eriophyidae): origin and invasion sources inferred from mitochondrial (16S) and
1293 nuclear (ITS) sequences. *Bulletin of Entomological Research*, **95**, 505–516.
1294 <https://doi.org/10.1079/BER2005382>
1295 Navia D, Novelli VM, Rombauts S, Freitas-Astúa J, Santos de Mendonça R, Nunes MA, Machado
1296 MA, Lin Y-C, Le P, Zhang Z, Grbić M, Wybouw N, Breeuwer JAJ, Van Leeuwen T, Van de Peer Y
1297 (2019) Draft Genome Assembly of the False Spider Mite *Brevipalpus yothersi*. *Microbiology Resource*
1298 *Announcements*, **8**, e01563-18. <https://doi.org/10.1128/mra.01563-18>
1299 Nei M, Kumar S (2000) *Molecular Evolution and Phylogenetics*. Oxford University Press, New
1300 York. <https://doi.org/10.1111/j.1471-0528.1976.tb00728.x>
1301 Ospina O, Massey S, Rodrigues JCV (2016) Reduced diversity in the bacteriome of the
1302 phytophagous mite *Brevipalpus yothersi* (Acari: Tenuipalpidae). *Insects*, **7**, 80.
1303 <https://doi.org/10.3390/insects7040080>
1304 Di Palma A, Tassi AD, Kitajima EW (2020) On some morphological and ultrastructural features of
1305 the insemination system in five species of the genus *Brevipalpus* (Acari: Tenuipalpidae). *Experimental*
1306 *and Applied Acarology*, **81**, 531–546. <https://doi.org/10.1007/s10493-020-00526-x>
1307 Peña JE, Santos K, Baez I, Carrillo D (2015) Physical post-harvest techniques as potential
1308 quarantine treatments against *Brevipalpus yothersi* (Acarina: Tenuipalpidae). *Florida Entomologist*, **98**,
1309 1169–1174. <https://doi.org/10.1653/024.098.0422>
1310 Pepato AR, Klimov PB (2015) Origin and higher-level diversification of acariform mites – evidence
1311 from nuclear ribosomal genes, extensive taxon sampling, and secondary structure alignment. *BMC*
1312 *Evolutionary Biology*, **15**, 178. <https://doi.org/10.1186/s12862-015-0458-2>
1313 Puillandre N, Brouillet S, Achaz G (2021) ASAP: assemble species by automatic partitioning.
1314 *Molecular Ecology Resources*, **21**, 609–620. <https://doi.org/10.1111/1755-0998.13281>
1315 Puillandre N, Lambert A, Brouillet S, Achaz G (2012) ABGD, Automatic Barcode Gap Discovery
1316 for primary species delimitation. *Molecular Ecology*, **21**, 1864–1877. <https://doi.org/10.1111/j.1365-294X.2011.05239.x>
1317 Puillandre N, Modica M V., Zhang Y, Sirovich L, Boisselier M-C, Cruaud C, Holford M, Samadi S
1318 (2012) Large-scale species delimitation method for hyperdiverse groups. *Molecular Ecology*, **21**, 2671–
1319 2691. <https://doi.org/10.1111/j.1365-294X.2012.05559.x>
1320 Quiros-Gonzalez M (1986) A systematic and phylogenetic analysis of the world genera of
1321 Tenuipalpidae Berlese (Acari: Tetranychoida). University of Maryland, College Park.
1322 Ragusa S, Athias-Henriot C (1983) Observations on the genus *Neoseiulus* Hughes
1323

1324 (Parasitiformes, Phytoseiidae). Redefinition. Composition. Geography. Description of two new species.
1325 *Revue Suisse de Zoologie*, **90**, 657–678.

1326 Rambaut A (2009) FigTree v1.4.4. *Institute of Evolutionary Biology, University of Edinburgh,*
1327 *Edinburgh*. <http://tree.bio.ed.ac.uk/software/figtree/>

1328 Robinson E, Blagoev G, Hebert P, Adamowicz S (2009) Prospects for using DNA barcoding to
1329 identify spiders in species-rich genera. *ZooKeys*, **16**, 27–46. <https://doi.org/10.3897/zookeys.16.239>

1330 Rodrigues JC V., Gallo-Meagher M, Ochoa R, Childers CC, Adams BJ (2004) Mitochondrial DNA
1331 and RAPD polymorphisms in the haploid mite *Brevipalpus phoenicis* (Acari: Tenuipalpidae).
1332 *Experimental and Applied Acarology*, **34**, 275–290. <https://doi.org/10.1007/s10493-004-0571-1>

1333 Ronquist F, Teslenko M, Van Der Mark P, Ayres DL, Darling A, Höhna S, Larget B, Liu L, Suchard
1334 MA, Huelsenbeck JP (2012) MrBayes 3.2: Efficient bayesian phylogenetic inference and model choice
1335 across a large model space. *Systematic Biology*, **61**, 539–542. <https://doi.org/10.1093/sysbio/sys029>

1336 Ros VIDD, Breeuwer JAJJ (2007) Spider mite (Acari: Tetranychidae) mitochondrial COI phylogeny
1337 reviewed: host plant relationships, phylogeography, reproductive parasites and barcoding.
1338 *Experimental and Applied Acarology*, **42**, 239–262. <https://doi.org/10.1007/s10493-007-9092-z>

1339 Rosenberg NA (2003) The shapes of neutral gene genealogies in two species: probabilities of
1340 monophyly, paraphyly, and polyphyly in a coalescent model. *Evolution*, **57**, 1465.
1341 <https://doi.org/10.1554/03-012>

1342 Rozas J, Ferrer-Mata A, Sánchez-DelBarrio JC, Guirao-Rico S, Librado P, Ramos-Onsins SE,
1343 Sánchez-Gracia A (2017) DnaSP 6: DNA Sequence polymorphism analysis of large data sets.
1344 *Molecular Biology and Evolution*, **34**, 3299–3302. <https://doi.org/10.1093/molbev/msx248>

1345 Sakamoto H, Matsuda T, Suzuki R, Saito Y, Lin J-Z, Zhang Y-X, Sato Y, Gotoh T (2017) Molecular
1346 identification of seven species of the genus *Stigmaeopsis* (Acari: Tetranychidae) and preliminary
1347 attempts to establish their phylogenetic relationship. *Systematic and Applied Acarology*, **22**, 91.
1348 <https://doi.org/10.11158/saa.22.1.10>

1349 Salinas-Vargas D, Santillán-Galicia MT, Guzmán-Franco AW, Hernández-López A, Ortega-Arenas
1350 LD, Mora-Aguilera G (2016) Analysis of genetic variation in *Brevipalpus yothersi* (Acari: Tenuipalpidae)
1351 populations from four species of citrus host plants (WJ Etges, Ed.). *PLOS ONE*, **11**, e0164552.
1352 <https://doi.org/10.1371/journal.pone.0164552>

1353 Sánchez-Velázquez EJ, Santillán-Galicia MT, Novelli VM, Nunes MA, Mora-Aguilera G, Valdez-
1354 Carrasco JM, Otero-Colina G, Freitas-Astúa J (2015) Diversity and genetic variation among *Brevipalpus*
1355 populations from Brazil and Mexico (WJ Etges, Ed.). *PLOS ONE*, **10**, e0133861.
1356 <https://doi.org/10.1371/journal.pone.0133861>

1357 Savitzky A, Golay MJE (1964) Smoothing and differentiation of data by simplified least squares
1358 procedures. *Analytical Chemistry*, **36**, 1627–1639.

1359 Shropshire JD, Leigh B, Bordenstein SR (2020) Symbiont-mediated cytoplasmic incompatibility:
1360 What have we learned in 50 years? *eLife*, **9**, 1–36. <https://doi.org/10.7554/eLife.61989>

1361 Skoracka A, Kuczyski L, Santos de Mendonça R, Dabert M, Szydło W, Knihinicki D, Truol G, Navia
1362 D (2012) Cryptic species within the wheat curl mite *Aceria tosichella* (Keifer) (Acari: Eriophyoidea),
1363 revealed by mitochondrial, nuclear and morphometric data. *Invertebrate Systematics*, **26**, 417–433.
1364 <https://doi.org/10.1071/IS11037>

1365 Srivathsan A, Meier R (2012) On the inappropriate use of Kimura-2-parameter (K2P) divergences
1366 in the DNA-barcoding literature. *Cladistics*, **28**, 190–194. <https://doi.org/10.1111/j.1096-0031.2011.00370.x>

1367 Staden R, Beal KF, Bonfield JK (1998) The Staden Package, 1998. In: *Bioinformatics Methods*
1368 *and Protocols*, pp. 115–130. Humana Press, New Jersey. <https://doi.org/10.1385/1-59259-192-2:115>

1369 Sterck, L., Billiau, K., Abeel, T., Rouzé, P., Van de Peer, Y. (2012) ORCAE: online resource for
1370 community annotation of eukaryotes. *Nature Methods* **9**, 1041. <https://doi.org/10.1038/nmeth.2242>

1371 Strimmer K, von Haeseler A, Salemi M (2009) Genetic distances and nucleotide substitution
1372 models. In: *The Phylogenetic Handbook* (eds Lemey P, Marco S, Vandamme A-M), pp. 111–141.
1373 Cambridge University Press, Cambridge. <https://doi.org/10.1017/CBO9780511819049.006>

1374 Tang CQ, Obertegger U, Fontaneto D, Barraclough TG (2014) Sexual species are separated by
1375 larger genetic gaps than asexual species in rotifers. *Evolution*, **68**, 2901–2916.
1376 <https://doi.org/10.1111/evo.12483>

1377 Tixier MS, Kreiter S, Ferragut F, Cheval B (2006) The suspected synonymy of *Kampimodromus*
1378 *hmiminai* and *Kampimodromus adrianae* (Acari: Phytoseiidae): morphological and molecular
1379 investigations. *Canadian Journal of Zoology*, **84**, 1216–1222. <https://doi.org/10.1139/Z06-108>

1380 Welbourn WC, Ochoa R, Kane EC, Erbe EF (2003) Morphological observations on *Brevipalpus*
1381 *phoenicis* (Acari: Tenuipalpidae) Including comparisons with *B. californicus* and *B. obovatus*.
1382 *Experimental and Applied Acarology*, **30**, 107–133.

1384 <https://doi.org/10.1023/B:APPA.0000006545.40017.a0>
1385 Wilcox TP, Zwickl DJ, Heath TA, Hillis DM (2002) Phylogenetic relationships of the dwarf boas and
1386 a comparison of Bayesian and bootstrap measures of phylogenetic support. *Molecular Phylogenetics*
1387 *and Evolution*, **25**, 361–371. [https://doi.org/10.1016/S1055-7903\(02\)00244-0](https://doi.org/10.1016/S1055-7903(02)00244-0)
1388 Yang C, Li Y-X, Yang X-M, Sun J-T, Xu X-N, Hong X-Y (2012) Genetic variation among natural
1389 populations of *Euseius nicholsi* (Acari: Phytoseiidae) from China detected using mitochondrial COXI
1390 and nuclear rDNA ITS sequences. *Systematic and Applied Acarology*, **17**, 171–181.
1391 <https://doi.org/10.11158/saa.17.2.3>
1392
1393